I.FAST

Innovation Fostering in Accelerator Science and Technology

Horizon 2020 Research Infrastructures GA n° 101004730

DELIVERABLE REPORT

Roadmap for Future Accelerators

MILESTONE: D5.2

Document identifier:	IFAST-D5.2
Due date of deliverable:	End of Month 40 (30 September 2024)
Report release date:	03/10/2024
Work package:	WP5: Strategies and milestones for accelerator research and technology
Lead beneficiary:	CERN
Document status:	Final

ABSTRACT

Summarizing 3.5 years of I.FAST activities and taking into account the worldwide state of the art in various domains of accelerator science, we present an R&D plan and step-wise approach towards ultimate hadron and lepton beams. Aside more mainstream topics, we review advances in photon science, nuclear science, neutron science, high-field magnet technology, and medical applications; sketch a strategy for intense positron sources; discuss past lessons and possible directions for crystalline beams; review the strategy and requirements for “beam chaser” colliders and EDM rings; discuss the roadmap for accelerator AI, and for accelerator-based quantum computing; and we survey the actual situation and future roadmap for green accelerators and for safe CO2-free energy production. Among the highlights are new radiation schemes, novel neutron sources, and nano-accelerators.

For more information on IFAST, its partners and contributors please see https://ifast-project.eu/

This project has received funding from the European Union's Horizon 2020 Research and Innovation programme under Grant Agreement No 101004730. IFAST began in May 2021 and will run for 4 years.

Delivery Slip

	Name	Partner	Date
Authored by	I. Agapov, R. Assmann, A. Ballarino, R. Bartolini, C. Carli, I. Chaikovska, U. Dorda, M. Fuchs, G. Franchetti, F. Hug, R. Ischebeck, B. Lorentz, V. Morozov, J. Olivares, H. Podlech, J. Resta Lopez, J. Rosenzweig, A. Sherjan, H. Tanaka, M. Vretenar, J. Yang, Y. Yuan, F. Zimmermann	CERN, DESY, GSI, GU Frankfurt, IHEP, IJCLab, IMP, INFN, KIT, MYRRHA, ORNL, PSI, RIKEN SPring-8, UCLA, U Valencia	30/09/2024
Reviewed by	M. Vretenar [on behalf of Steering Committee]	CERN	03/10/2024
Approved by	Steering Committee		03/10/2024

TABLE OF CONTENTS

1 EC STRATEGY AND ROADMAP FOR ACCELERATORS 4
2 MORE SUSTAINABLE AND MORE EFFICIENT ACCELERATORS 5
3 ACCELERATORS SOLVING THE ENERGY PROBLEM 10
4 FUTURE COLLIDERS 12
5 HIGHER-FIELD ACCELERATOR MAGNETS 13
6 HIGHER POWER HADRON MACHINES 16
7 FASTER ACCELERATOR CONSTRUCTION 17
8 ACCELERATOR AI: BETTER DESIGN, OPERATION & PHYSICS 18
9 SYNERGETIC AND COMBINED ACCELERATOR APPLICATIONS 18
10 CRYSTALLINE BEAMS 19
11 STORAGE RINGS FOR QUANTUM COMPUTING 20
12 POSITRON SOURCES AND POSITRON SCIENCE 22
13 PHOTON SOURCES INCLUDING THZ SOURCES 24
14 NEUTRON SOURCES 31
15 COLLISIONS IN A CO-MOVING FRAME 35
16 COMPACT HIGH-PRECISION STORAGE RINGS 37
17 MEDICAL ACCELERATORS 38
18 COMPACT ADVANCED INJECTORS 40
19 NANO-ACCELERATORS 42
20 CONCLUSIONS AND RECOMMENDATIONS 43
REFERENCES 45
ANNEX A: CONCLUSIONS FROM IBIF2024 DISCUSSION 46
ANNEX B: PHOTOGRAPHS FROM IBIF2024 47

Executive summary

This report summarizes the presentations and discussions from the iFAST brainstorm and roadmap workshop in Frankfurt, which reviewed the accomplishments during 3.5 years of iFAST activities and recent worldwide advances art in various domains of accelerator science [1], plus other related discussions and developments.

In particular, we review ongoing facility constructions and upgrades along with longer-term goals in the areas of photon science, nuclear science, particle physics, and neutron science, along with recent and planned progress in accelerator technologies, including high-field magnets, and greatly improved energy efficiency. The result is an R&D plan and a step-wise approach towards ultimate hadron and lepton beams. We also sketch a strategy for intense positron sources; discuss past lessons and possible directions for crystalline beams; review the strategy and requirements for new synchrotron radiation sources, as well as for co-moving nuclear colliders and EDM rings; we discuss the roadmap for accelerator AI, accelerator-based quantum computing, and nano-accelerators; we also report unfolding advances in medical accelerators; finally, we survey the actual situation and future roadmap for greener accelerators and for safe accelerator-based CO2-free energy production.

1 EC Strategy and Roadmap for Accelerators

The EC recognizes particle accelerators as a critical technology and key component of European "big science". Competition for funding is increasing. Future EC calls will be increasingly competitive. For the accelerator community, it is important to show the integration of roadmaps from different partners, including the roadmap developed here, in the frame of iFAST.

Figure 1 illustrates that roadmaps are a growth business. The dream of funding authorities is a single roadmap that specifies the accelerator R&D and for future accelerators in one piece. One roadmap requires a set of common and over-arching goals, which clearly crystallized at this workshop: greater sustainability, accelerator-based energy generation, better performance for users (brightness, luminosity, beam power, energy, gradients, greater compactness, harnessing AI, …), new areas of applications like accelerator-based quantum computing or dual-species rings, serving wider user communities, synergetic operation, and faster plus more economical construction.

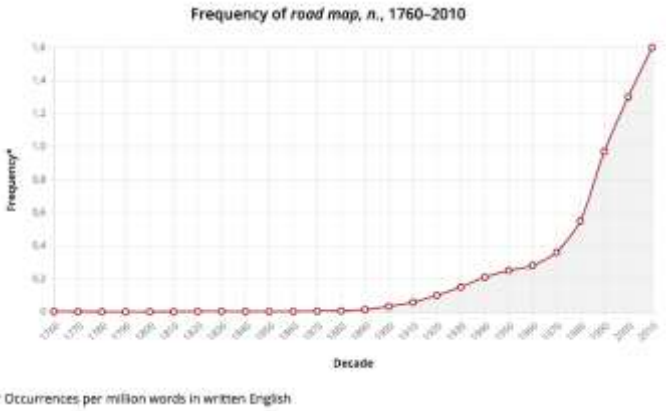

Figure 1: The use of the term "roadmap" in written English [from the presentation of R. Assmann].

2 More Sustainable and More Efficient Accelerators

Both hadron and lepton accelerators are making dramatic leaps in energy efficiency while also increasing the accelerator performance. This is achieved by new technologies including auxiliary systems, such as power supplies with energy storage, high-field or higher-temperature superconducting magnets, advanced undulator devices, better integration and better adapted subsystem parameter choices, new concepts such as multi-bend achromatic lattices plus permanent magnets for light sources, nanobeam crab-waist collisions, and energy recovery linacs.

Figures 2-3 illustrate the merits of the planned upgrade of the synchrotron light source SPring-8 to Spring-8-II, operating at lower the beam energy, with a different beam optics, and using more advanced undulator magnets. With the upgrade, the photon brilliance increases by almost two orders of magnitude and all this with only half of the electrical power consumption (Fig. 4).

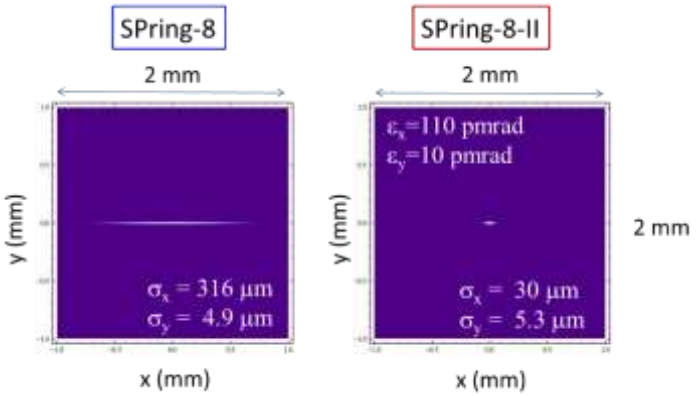

Figure 2: Comparison of photon source size in the existing SPring-8 ring (left) and the future SPring-8-II ring (right) [from the presentation of H. Tanaka].

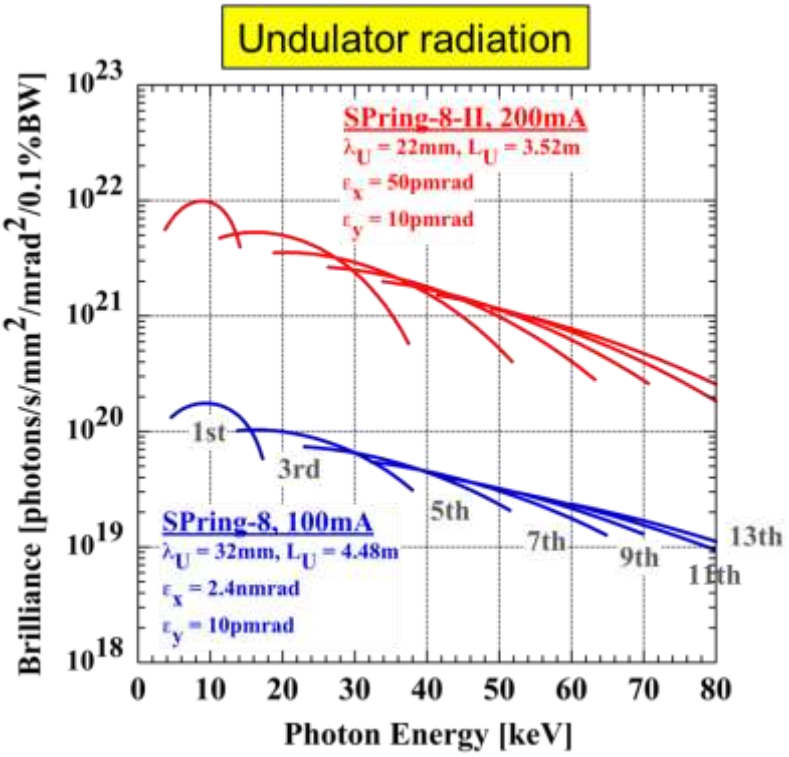

Figure 3: X-rays provided by SPring-8-II compared with the present SPring-8 [from the presentation of H. Tanaka].

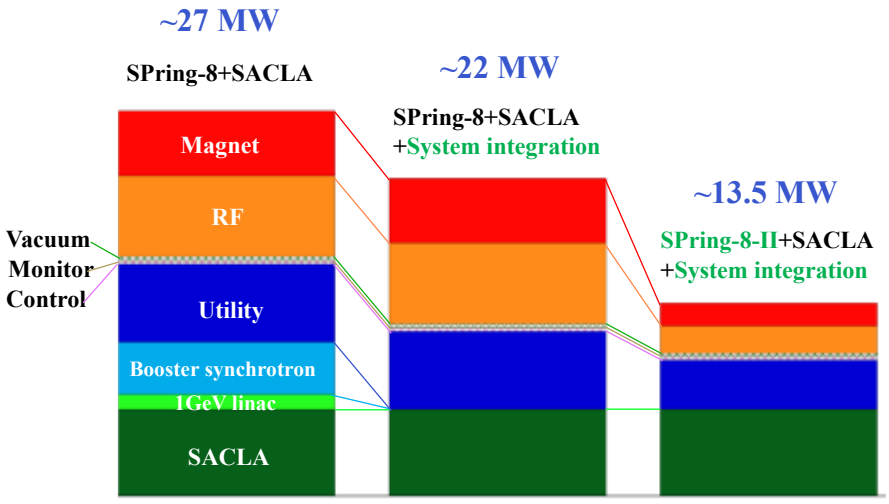

Figure 4: Change in the electrical power consumption of the RIKEN SPring-8 complex after system integration (combined linacs) and after implementing the SPring-8-II upgrade [from the presentation of H. Tanaka].

Also XFELs are getting more energy efficient. A point in case is the planned upgrade of SACLA to SACLA-II (Fig. 5).

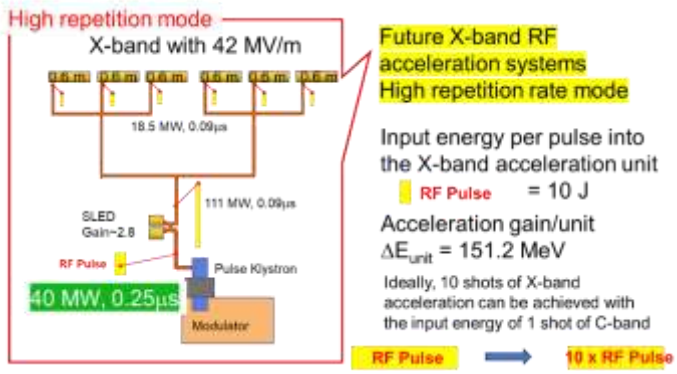

Figure 5: Upgrade from SACLA to 10x more efficient SACLA-II by changing from C-band to X-band [from the presentation of H. Tanaka].

The proposed plasma injector for the future PETRA IV light source would greatly reduce the electrical power consumption, by an order of magnitude from close to 3 MW to ~0.3 MW, compared with a conventional injector chain consisting of LINAC II and the DESY IV synchrotron (Fig. 57).

Similar progress is seen in nuclear physics facilities. Table 1 presents the enormous power and energy saving thanks to novel poser supplies with energy storage in case of the fast cycling BRing at HIAF, where energy is transferred between magnets and a capacitor tank.

Table 1: Power requirement for the BRing and for the entire HIAF complex with conventional power supplies and using novel power supplies with energy storage [from the talk of J. Yang].

Power requirement (MVA)	Conventional	Energy storage
BRing bendng magnet	**180**	**15**
BRing quadruple magnet	**50**	**6**
Total of BRing	250	41
Total of HIAF	297	88

Figure 6 illustrates the improved energy efficiency already achieved by changing the beam optics and ring parameters from KEKB to SuperKEKB. Much higher luminosity is achieved at lower beam current or lower electrical power consumption (dominated by synchrotron radiation).

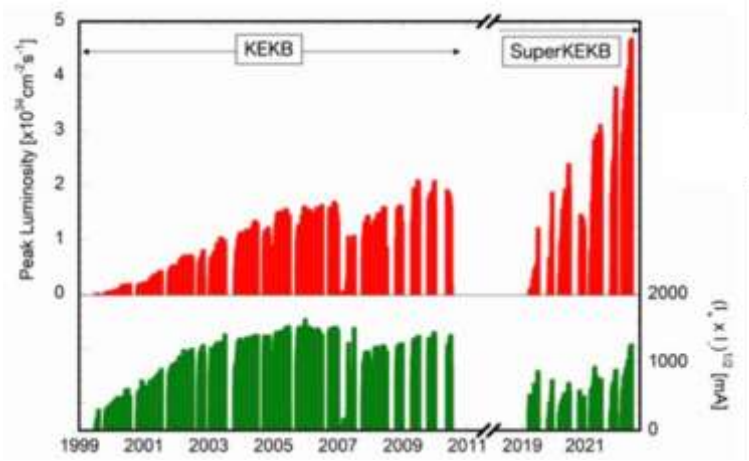

Figure 6: Change in the peak luminosity performance after upgrading from KEKB to SuperKEKB (red histogram, top) and the average beam current (geometric mean of electron and positron current, green histogram, bottom) versus the year [from a presentation of M. Masuzawa].

Energy efficiency also is a key figure of merit for future hadron linacs. All proton linacs use room-temperature front ends, like RFQs and Alvarez or CH/IH linacs. At energies above 100 MeV SC linacs are common. Duty factor and beam current determine the optimum transition energy between room-temperature copper structures and superconducting linear accelerators. This optimum transition is apparent from Fig. 7. The only outlier is IFMIF, with a use of SC technology from an unusually low energy of about 2 MeV.

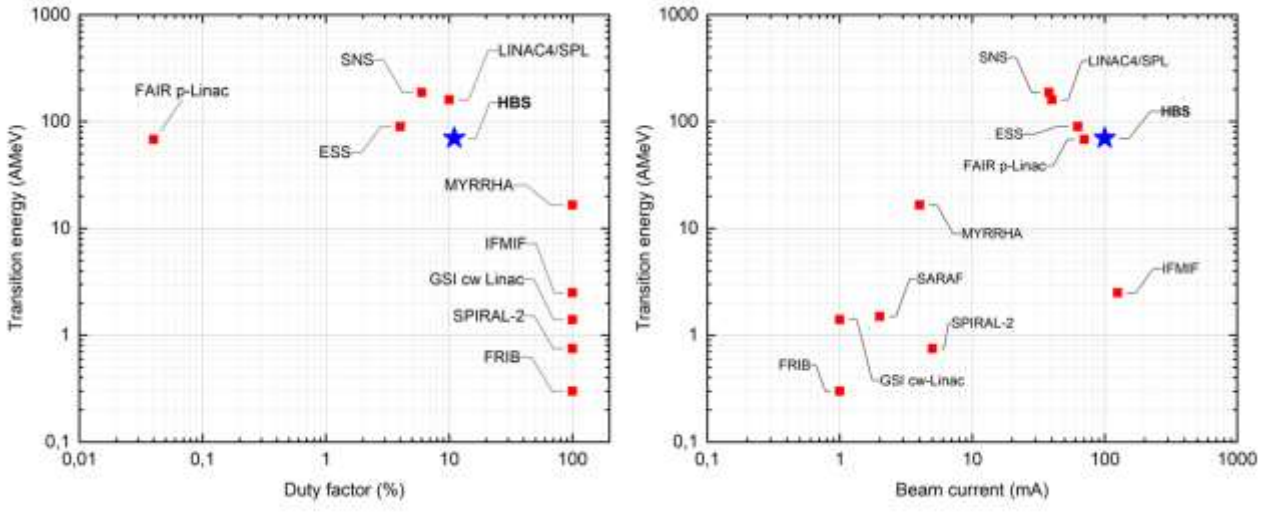

Figure 7: Energy-optimized transition energy between room-temperature front ends and higher-energy SC linacs [from the presentation of H. Podlech].

Figure 8 presents the example of the future high brilliance neutron source HBS, with a final beam energy of 70 MeV, comprising a drift-tube linac made from 40 room-temperature CH-cavities, SSA

amplifiers of 100-600 kW, with a peak loss 100 kW/m or a thermal loss 25 kW/m (25% duty factor), and a total RF power of 16 MW. More than 50% of the RF power is transferred to the beam.

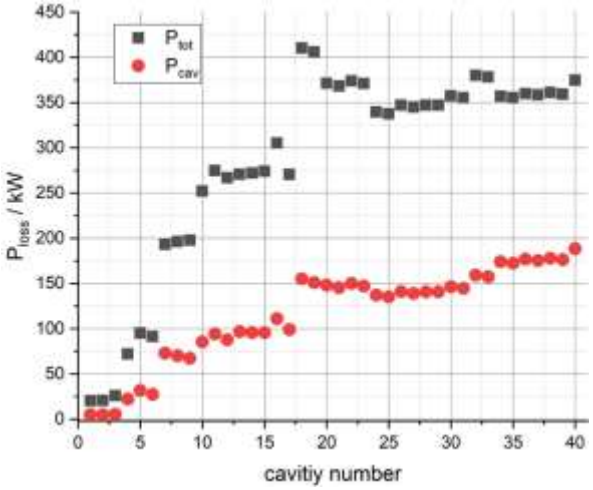

Figure 8: Total RF power and power lost in the room-temperature cavities for the HBS drift tube linac with 25% duty factor [from the presentation of H. Podlech].

By recovering the beam energy, energy recovery linacs (ERLs) hold the promise of much higher energy efficiency than conventional single pass linacs. The worldwide ERL landscape is shown in Fig. 9. Possible ERL applications comprise every experiment/process which needs a high cw beam current and does not use too destructive targets. Examples are light/gamma beam production (Fully Coherent Light Sources, ERL based EUV-FELs for lithography, Laser Compton Backscattering for nuclear physics, etc.), Strong Hadron Cooling in the Electron Ion Collider (EIC), providing electron/positron or even muon beams for high luminosity colliders, and high precision nuclear or particle physics experiments in combination with gas-jet targets as in the case of MESA in Mainz. MESA is one of 3-4 ongoing ERL activities and the only user facility. MESA is in the commissioning state of injector; the first beam to the MESA experiments is expected in 2025. While CBETA in the US and bERLinPro in Germany are both on hold, two other, new ERLs, PERLE in Paris and BriXSinO in Milano/Italy, will start operation, at higher intensities, in 2028-2030, if these projects receive the full funding. BriXSinO, with 40 MeV beam energy and 225 kW beam power in ERL operation, features a dogbone design and will allow for experiments with THz radiation and the Compton backscattering of photons. The timeline for the BriXSino construction is 2023-2028, with first beams from the injector by end 2025.

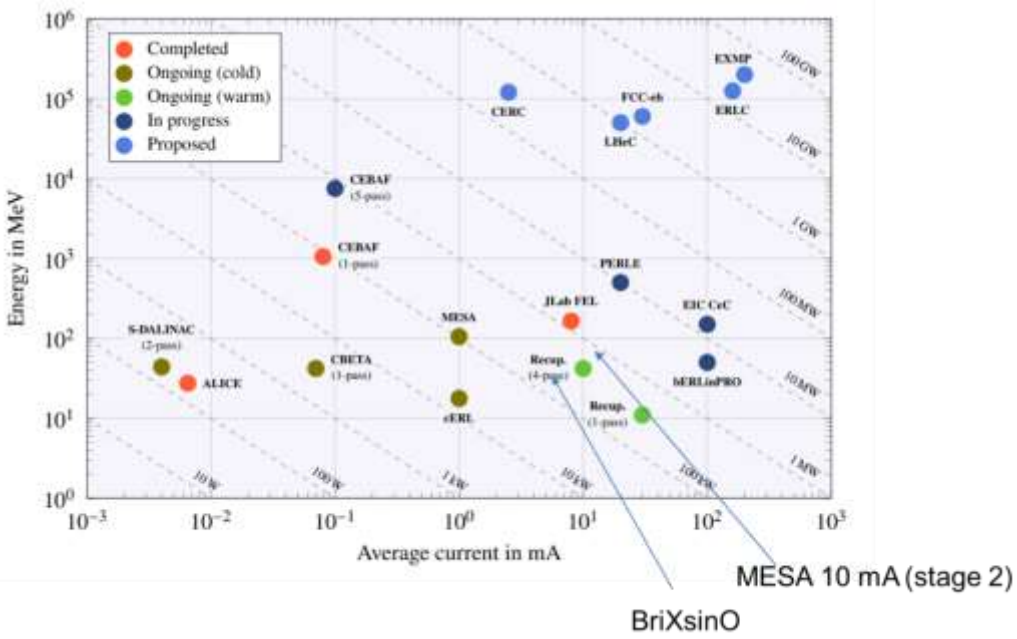

Figure 9: ERL landscape in 2024 with MESA ad BriXsinO [from the presentation of F. Hug].

Storage rings are intrinsically energy efficient, in particular if they employ cw SC radiofrequency systems, or SC magnet systems, and since they reuse the beam over very many turns. The efficiency of ring colliders can further be boosted by accommodating several collision points and experiments, such as for the Future Circular Collider (see below).

3 Accelerators solving the Energy Problem

Instead of making accelerators only more energy-efficient, novel accelerators can also be used for energy generation. Possible options include accelerator-driven subcritical reactors, including ones driven by photons from the LHC-based Gamma Factory, and accelerator-based fusion.

Various bodies like IPCC, IAEA, IEA have stated that nuclear energy is a crucial technology to reach CO_2 neutrality by 2050. Average lifecycle emissions are 6-10 g CO_2[eq]/kWh, which is comparable to hydropower or windmills, and 20x less than natural gas, or 35x lower than coal. By end 2023, 417 nuclear reactors were in operation in 31 countries, and 58 new ones under construction. Electrical power contribution from nuclear energy is about 10% worldwide, with 19% for the USA, 25% for the EU. In November 23 at COP28, 22 countries have committed to nuclear energy in their energy mix.

Unfortunately, fission generates high level radioactive waste. 1 ton of nuclear fuel produces electricity for 100,000 families for 4.5 years. After 4.5 years the spent nuclear fuel contains 94.7% of resources we can recycle (U+Pu), 5.1% of nuclear waste with low radiotoxicity (FP's). and 0.2% of high radiotoxicity nuclear waste. The decay time of the radioactivity with different forms of waste processing is shown in Fig. 10.

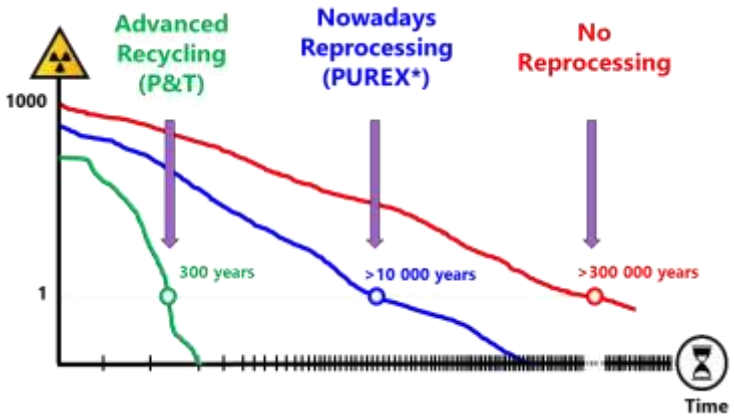

Figure 10: Decay time of reactor waste radioactivity after different processing and recycling steps [from the presentation of U. Dorda].

Accelerator-driven systems (ADS) with subcritical reactors hold several promises: (1) if the accelerator stops, the reactor "stops" (hence, it is intrinsically safe), (2) a reduced radio-toxicity of the waste, and (3) better use of the resources. ADS offers the most effective transmutation of radioactive waste with a rate of 35 kg/TWh, about 10 times more than a fast reactor could achieve.

ADS accelerators should provide proton beams with MW class average beam power, with an energy above 500 MeV, mA current, and preferably in CW beam mode. They must support the reactor cycle operational schedule (e.g., 90 days cycle) and be of highest reliability to avoid thermal stress on reactor components, and ensure uptime needed for the transmutation.

The two most advanced projects in the world are MYRRHA in Belgium, whose first stage (100 MeV) is under implementation, and CiADS in China, where the complete facility is under construction.

MYRRHA, sketched in Fig. 11, is an ADS technology demonstrator at pre-industrial scale, which can also serve as a flexible irradiation facility.

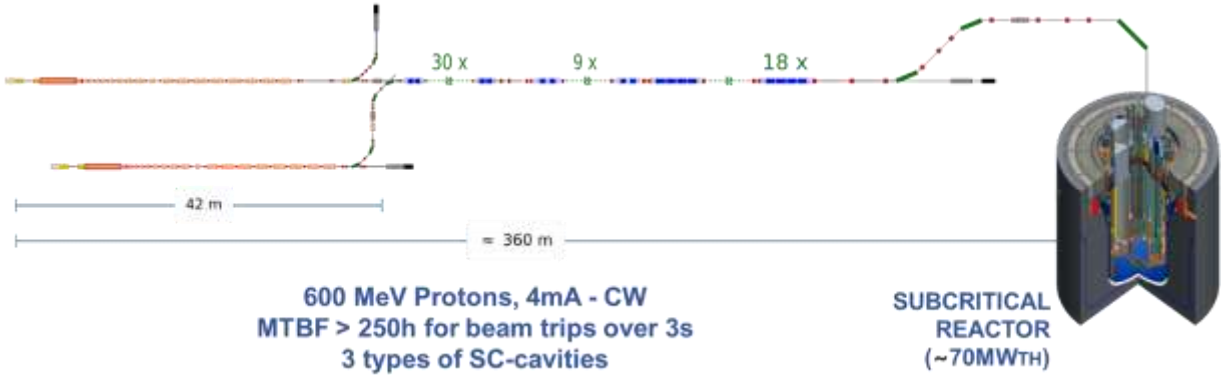

Figure 11: schematic of MYRRHA at SCK CEN in Belgium [from the presentation of U. Dorda].

The first stage of MYRRHA is MINERVA, delivering a 100 MeV beam by end 2027, with 1 injector and 1 SC cavity type. MINERVA will allow testing the reliability concepts (RF-fault tolerance). Normal conducting CH-cavities at 176 MHz will accelerate up to 17 MeV. This is followed by two 352.2 MHz single spoke cavities per 2 K cryomodule.

The CiADS, under construction in China, will send 0.5 GeV, 2.5 MW proton beams from a SC linac into a sub-critical lead-bismuth eutectic (LBE) fast reactor.

More advanced accelerator-based energy-generation schemes include UCLA's Beam Chaser [2], where a velocity differential leads to two beams chasing each other and colliding in a moving frame to produce directional products at manageable collision angles, which can include fusion events. Extracting energy without generating neutron is possible by selecting aneutronic fusion reaction like $p + B \rightarrow 3\alpha$, whose cross section peaks at 600 keV. One can harness the α energy via deceleration. Table 2 presents example parameters for a fusion accelerator based on the beam-chaser concept [2]. With a beam current of 500 A, close to 10 kW of power is generated; see Table 2.

Table 2: Beam parameters for a $p + B \rightarrow 3\alpha$ fusion accelerator [from the presentation of J. Rosenzweig].

Proton kinetic energy	19.2 MeV
Boron kinetic energy	137 MeV
Rest frame energy available	673 keV
Bend radius (1 T)	1.12 m
Solenoid B-field	2.2 T
Beam current	500 A (!)
Beam size in interaction	60 um
Interaction length (slip limited)	10 m
Interaction rate	5E15/sec
Fusion power	7 kW

4 Future Colliders

Various future circular or linear electron-positron collider Higgs factories, 100 TeV scale hadron colliders, and muon colliders at 10s of TeV collision energies are proposed. At present, SuperKEKB in Japan holds the collider luminosity world record and has achieved the smallest "beta-star" ever for any operating collider, of 0.8 mm. In the US, the Electron-Ion Collider has been approved and is under construction.

The planned Future Circular Collider (FCC) at CERN in Europe consists of two phases, as indicated in Fig. 12. The first phase is a highest-luminosity e^+e^- collider, FCC-ee, serving as Higgs, electroweak and top factory. In a second phase this will be followed by an energy frontier hadron collider, FCC-hh. A similar two-stage project CEPC/SPPC is under study in China.

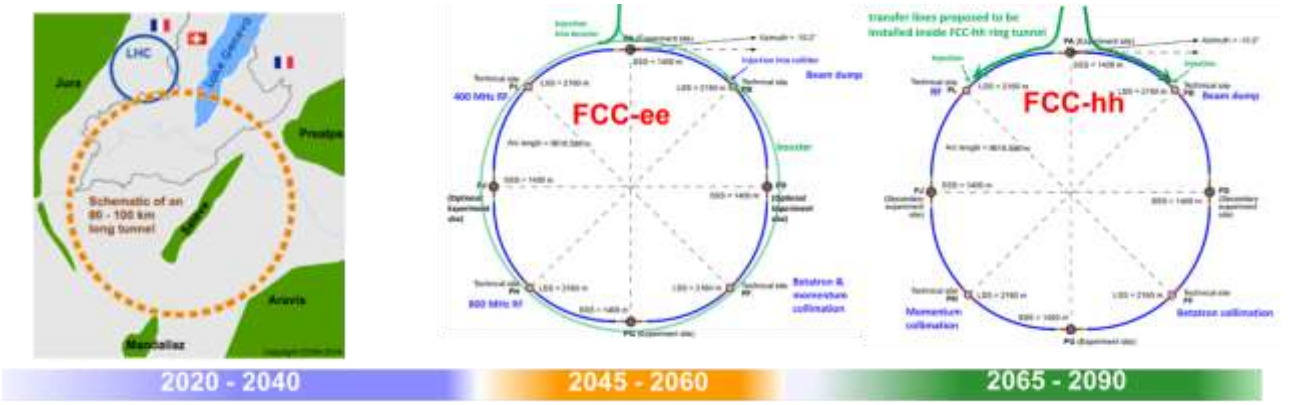

Figure 12: Rough placement, layouts, and timeline for the FCC integrated programme [from the presentation of F. Zimmermann].

5 Higher-Field Accelerator Magnets

A future hadron collider will require high-performance SC magnets. Superconductors used or considered for high-field magnets are shown in Fig. 13. The LHC, with a dipole field above 8 T, and all previous hadron colliders used Nb-Ti conductor. The HL-LHC is the first machine utilizing Nb_3Sn quadrupole magnets in an accelerator (aside an earlier Nb_3Sn wiggler at SPring-8 and a Nb_3Sn magnet of the HIAF ion source), with a peak field inside the coil of about 11.4 T. Efforts of magnet R&D focus on Nb_3Sn magnets and High-Temperature Superconductor (HTS). Prototype Nb_3Sn dipole magnets presently being developed in Europe are shown in Fig. 14.

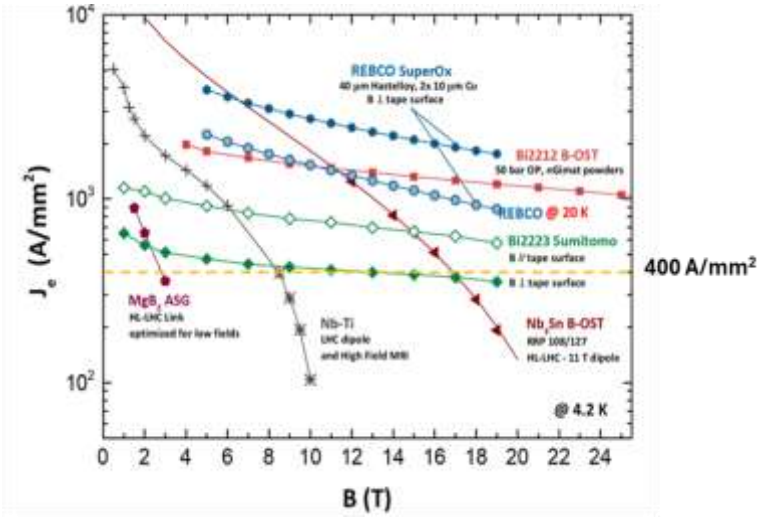

Figure 13: Critical current as a function of magnetic field, for various actual and possible high-field magnet superconductors [from the presentation of A. Ballarino].

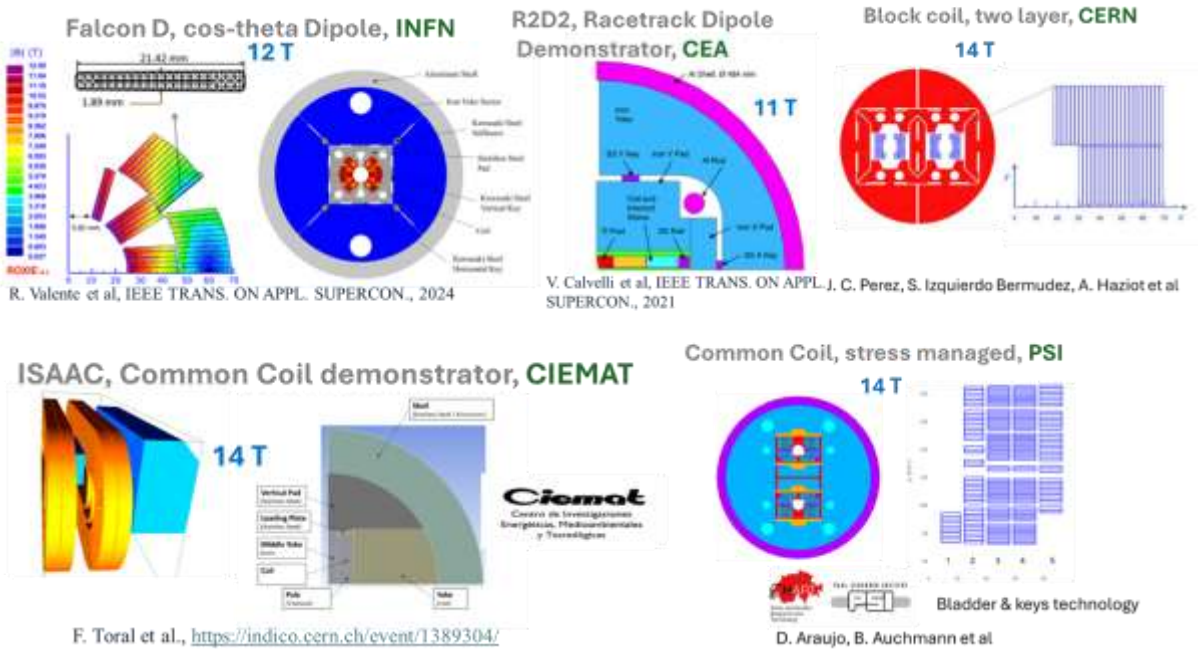

Figure 14: Ongoing validation of Nb_3Sn magnet technology on 11 T- 14 T demonstrator dipoles at major institutes and organisations in Europe [from the presentation of A. Ballarino].

HTS is an enabling technology for higher fields (> 16 T), and would enable a sustainable technology for future accelerators. Advantages are its high critical current density, high critical field (Fig. 15), higher operating temperature (less cryogenic power), no training, thermal stability, etc.. To exploit its potentials and bridge the technological gap with respect to Nb-Ti and Nb_3Sn, rigorous R&D and innovation are required, both on conductor and magnets. Focus in Europe is on REBCO. Recently, also work on Iron Based Superconductors has started, which is a conductor favoured for a future hadron collider in China (SPPC).

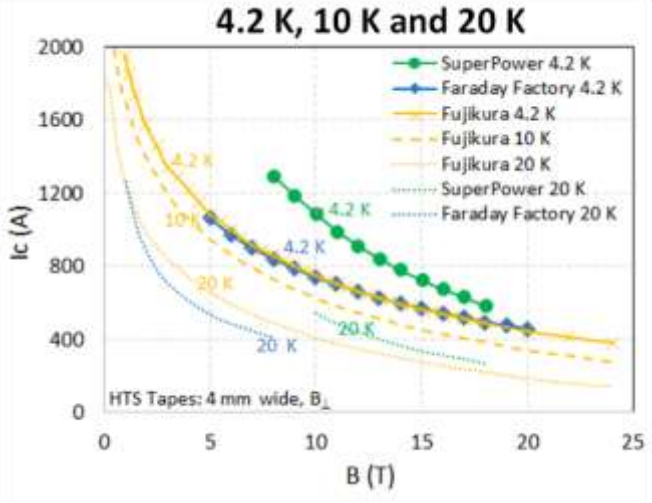

Figure 15: Critical current density versus magnetic field for HTS tapes at three different temperatures and from three different producers [from the presentation of A. Ballarino].

HTS magnet development has important synergies with other applications for society, such as fusion, medical applications, electrical applications including power transmission, aircraft and marine use. For the UK fusion effort, large scale procurement of HTS (~10,000 km/year) is expected to begin in 2028.

The even much more ambitious REBCO conductor production plan from the Chinese company Shanghai Superconductors is illustrated in Fig. 16. For REBCO it is possible to tailor the electrical properties, by introducing artificial pinning centers or microstructures. The microstructures that produce the best critical current density J_c performance are not the same at high and low temperatures. One can finetune the production so as to optimize the in-field performance at the desired operating temperature, e.g. 4.2 K or 30 K or 77 K. Also, the anisotropy can be adjusted. Ongoing collaboration on REBCO magnets includes CERN, CEA, PSI, and KIT.

Figure 16: REBCO tape production plan and production facilities of Shanghai Superconductors [from the presentation of A. Ballarino].

It is well known that irradiation may degrade the properties of superconductors (e.g., doi: 10.1088/1361-6668/ac1523). GSI plans to investigate and quantify the effect of heavy ion irradiation on HTS tapes, such as on critical current and magnetization. For these studies, the GSI can provide a wide variety of heavy ions, i.e., carbon, argon, uranium, at different fluences and energies .

Finally, work in Europe on Iron-Based Superconductor (IBS) had started within a CERN-SPIN collaboration in November 2023. IBS allows for both wire and tape. IBS wires can be produced with the known scalable Powder-In-Tube process at potentially low cost. The goal of CERN-SPIN collaboration is to produce a multi-filamentary IBS wire with target current density $J_c \geq 10^3$ A/mm^2 at 20 K. The IBS conductor Ba-122 (Ba1-xKxFe2As2) has a critical temperature of $T_c \sim 38$ K, and a critical field H_{c2} at 20 K exceeding 70 T; see Fig. 17.

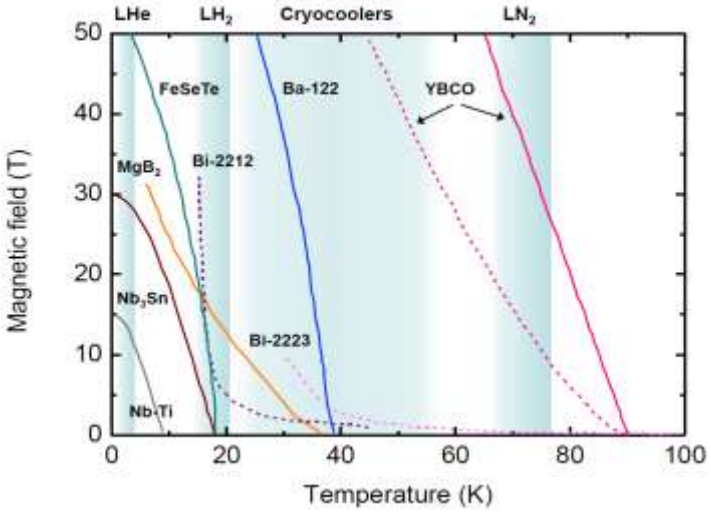

Figure 17: Different types of conductors, including the IBS conductor Ba-122, in the magnetic field / temperature landscape [from the presentation of A. Ballarino].

6 Higher Power Hadron Machines

The compact Ultra rapid Cycling Synchrotron (UCS) under development in China will push beam power by increasing the repetition rate to several hundred Hz. Figure 18 illustrates how this rate compares with other high-power hadron beam facilities, such as FAIR, CSNS, or J-PARC. UCS will have a circumference of about 120 m. The main challenges are the vacuum chamber because of the eddy currents etc., and the fast-cycling pulsed power supply.

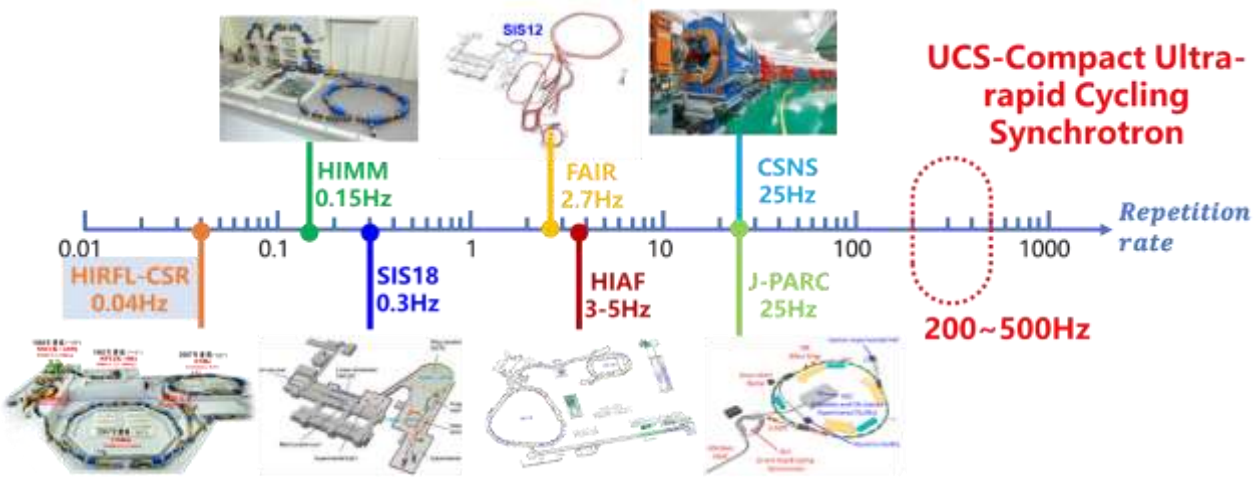

Figure 18: The landscape of high-power hadron beam facilities and their respective repetition rates [from the presentation of J. Yang].

7 Faster Accelerator Construction

Additive manufacturing finds ever wider application in the construction of accelerator components. Figure 19 shows the additive machining of a stainless-steel tank and copper electrodes for a high-power 704 MHz hadron-linac prototype “CH” structure at GSI/FAIR.

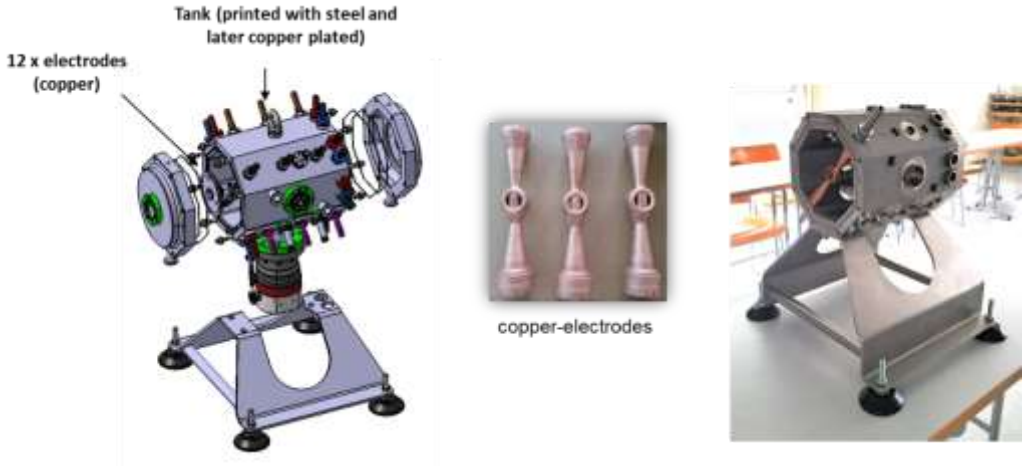

Figure 19: High-power RF structures for ion accelerators produced by (3D) additive machining [from the presentation of R. Assmann].

GSI, together with the IWS Fraunhofer Institute, has also produced a Fast Faraday Cup (FFC) made by 3D printing of copper. This FFC is the first ever additively manufactured RF beam diagnostic component. Suppression of secondary electron emission "by design" has also been demonstrated for this device.

Machines with fast ramping rates require thin wall vacuum chambers for all magnets to keep eddy currents at a tolerable level. For the HIAF fast cycling booster synchrotron BRing, a thin-wall (0.3 mm) stainless-steel chamber supported internally by 4-mm thick ceramic rings with Ti-alloy lining was chosen, as is illustrated in Fig. 20 (left picture). The actual implementation is in the form of TC4 cages (right picture) manufactured by 3D-SLM (Selective Laser Melting), which offers a high yield strength with 912 MPa, a low outgassing rate, high reliability, ease of manufacturing, and low cost.

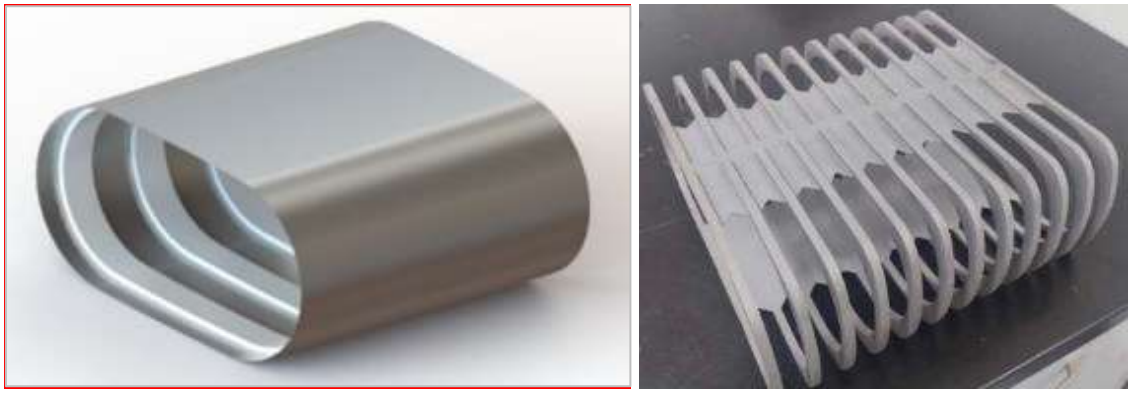

Figure 20: HIAF BRing's thin-wall vacuum chamber supported by ceramic rings; a conceptual view is shown on the left; the actual "TC4 cage" manufactured by 3D-SLM is illustrated on the right [from the presentation of J. Yang].

8 Accelerator AI: better design, operation & physics

In the field of accelerators, AI can help with simulations and modelling, data analysis, accelerator operations, and large language models. Taking as an example the Argonne wakefield accelerators, AI surrogate models have sped up multiobjective genetic optimization by a factor 1,000,000. Bayesian optimization has been used to maximize FEL photon pulse energy, incorporating safety constraints (PSI) and/or beam dynamics knowledge (SLAC).

A generic optimization framework is part of the Efficient Particle Accelerator (EPA) project at CERN, where the development focus is on automation to increase efficiency, reproducibility, flexibility and performance. Anomaly detection, 6-dimensional reconstruction of beam distribution, and virtual diagnostics are other examples of AI application in the accelerator field.

In general, machine learning is a natural way to approach problems. Applications from other areas of science and industry can be adapted to the accelerator domain. Large language models are likely to find fascinating applications, including for fully automated open-ended scientific discoveries.

9 Synergetic and Combined Accelerator Applications

The High-Intensity Heavy Ion Accelerator Facility (HIAF) and China Initiative Accelerator Driven System (CiADS) are constructed on the same campus in Huizhou City, Guangdong province. In the future the China advanced NUclear physics research Facility (CNUF) will join the two facilities as seen in Fig. 21. Radioactive beams produced by protons from CiADS can be post-accelerated in the upgraded HIAD.

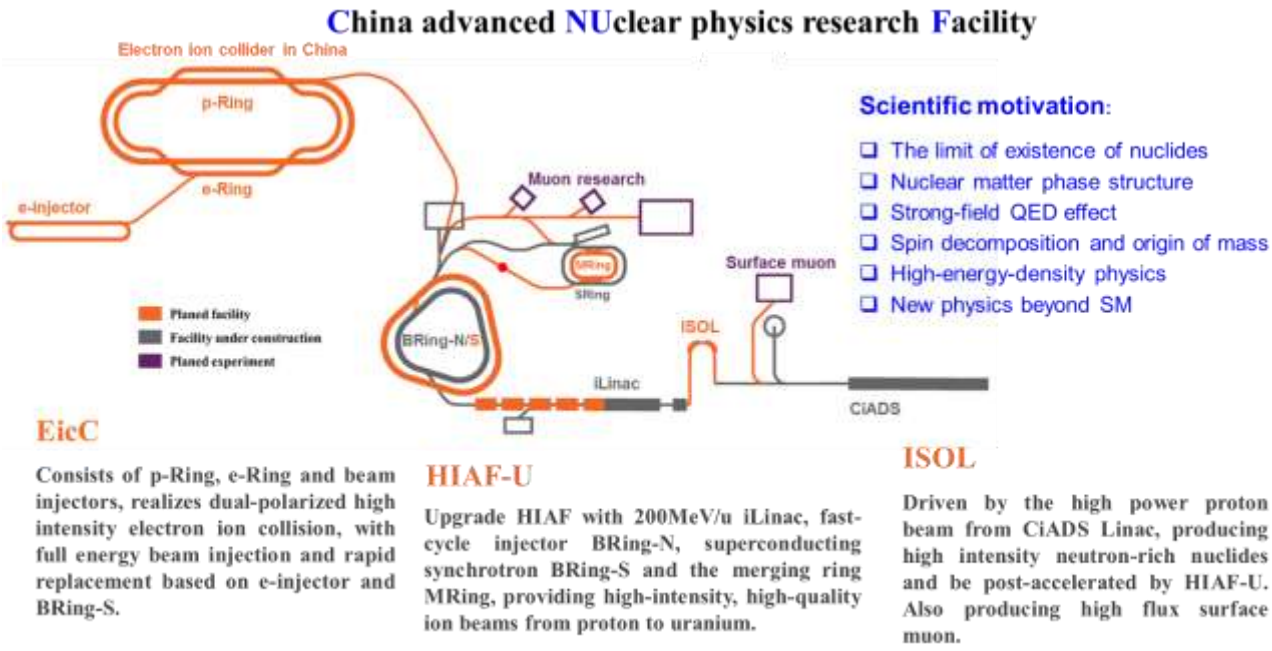

Figure 21: CNUF as a combined upgrade of HIAF and CiADs [from the presentation of J. Yang].

10 Crystalline Beams

About 20 years ago, major efforts around the world attempted to create and observe crystalline beams, e.g. at TSR in Heidelberg, ESR at GSI, ASTRID in Arhus, and S-LSR in Kyoto. CRYRING is another candidate facility, now also installed at GSI. These attempts were inspired by earlier observations of a Schottky signal anomaly at NAP-M in Novosibirsk and theoretical predictions. More than half of these machines observed evidence for an ordered 1D state, with inter ion distances of the order of several cm. All signs of 1D ordering were achieved with electron cooling, while laser cooling at TSR and ASTRID did not result in any similar ordered state; see Table 3. Only the PALLAS electrostatic ring, with very low particle energy (1 eV) produced true 1D, 2D and even 3D crystalline states.

Table 3: Storage rings which hunted for crystalline beams [from the presentation of B. Lorentz].

	NAP-M	TSR	ASTRID	ESR	CRYRING	S-LSR	PALLAS
E in MeV/u	65.7	1.9	0.00417	360	7.4	7	1eV
L in m	47.25	55.4	40	108.36	51.63	22.557	0.361
γ	1.07	1.002	1.00000444	1.384	1.00789	1.00746	
γT	1.18	2.96	4.34	2.67	2.33	1.41	
Nsp	4	2	4	6	6	6	800
Qx/Qy	1.352/1.2	2.57/2.21	1.38/1.32	2.3/2.3	2.3/2.3	1.6/1.2	60
Ion	p	7Li+	24Mg+	197Au79+	129Xe36+	p	24Mg+
Cooling	EC	LC	LC	EC	EC	EC	LC
Tx,y/Tz in K	50/1	--/3	50/0.001	27/18	50/18	9/1.5	1.5/0.3
N0 anomaly	2.00E+07		5.50E+08	4000	1000-10000	2000	
N0 (1D to 2D)	6.00E+06	1.40E+07	1.10E+06	7.90E+06	4.70E+06	3.20E+06	
Observation	Schottky anomaly	Indirect transverse cooling	Schottky anomaly	1D ordering	1D ordering	1D ordering	1D/2D/3D crystalls

It is proposed and planned to resume crystalline beam studies at the ESR, where now both electron and stochastic cooling systems are available.

11 Storage Rings for Quantum Computing

Quantum computing is a promising technology relying on fundamental principle of quantum mechanics such as qubit entanglement lacking classical analogues. Two of the greatest challenges are the quantum coherence time and the scalability, that is the ability to increase the number of qubits without exponential increase in the cost of resources.

In a spin transparent storage, the spin transformation in one turn around the ring is a unit operator, i.e., no net spin rotation. A Figure-8 ring topology is the most natural example, and the unit spin transformation here is independent of energy.

The benefits of this approach are a large number of qubits that can be stored in ring, long quantum coherence times of over an hour, and the lack of strict thermal constraints by using spin quantum properties only and not relying on quantum effects of particle motion and inter-qubit interaction. The set up can also be used as a quantum sensor or part of quantum memory. A practical realization is sketched in Fig. 22. The initial spin states of two or more $171Yb^{+}$ ions are prepared in an ion trap in a standard way. The preparation includes cooling and entanglement of the ions playing the role of qubits. The act of entanglement serves as an application of a two-qubit gate. Some of the qubits are extracted from the ion trap and injected into the storage ring. Their places in the ion trap are then refilled by newly injected ions, which are again prepared and optionally entangled with each other and the old qubits remaining in the trap from the earlier step. The process continues as needed. Once the necessary number of qubits is present in the ring, they are acted upon by single-qubit gates determined by the desired quantum computation algorithm. The final states are next read-out. The single-qubit gates and the readout procedure are implemented using standard techniques of laser-induced Rabi state transitions and fluorescence. This sequence of steps constitutes a quantum operation.

Table 4 illustrates the projected superior performance of a storage-ring based quantum computer.

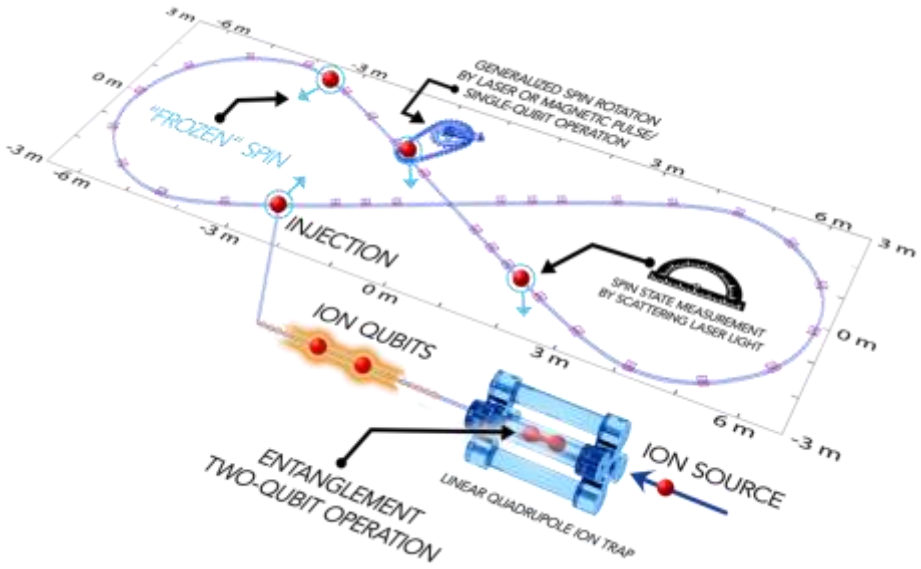

Figure 22: A spin transparent storage ring with entangled ion pairs as quantum computer [from the presentation of V.S. Morozov].

Table 4: Comparison of storage-ring based quantum computer with alternative approaches [from the presentation of B. Lorentz].

	Storage Ring (projected)	Neutral Atoms	SC Qubits	Trapped Ions	Photonics
Number of Qubits	10-10^5	280	127	32	216
Coherence Time	~3 hours	1.5 s	1 ms	5500 s	-
Measurement Fidelity	> 0.99	0.998	0.999	0.9993	0.98
Gate (Operation) Time	~10 ns	200 µs	4 ns	1.6 µs	-
One-Qubit Gate Fidelity	> 0.99	0.999	0.9992	0.999999	0.986
Two-Qubit Gate Fidelity	TBD	0.993	0.995	0.997	0.93

A small-scale prototype is posed. The ring circumference is determined by the number of stored qubits, not by the electric field strength limitation. To test key concepts and address open questions, a demonstration experiment could be the next step, with ring size significantly scaled down, say, by a factor of ~10, to a circumference of a few meters. This ring could still accommodate several hundred qubits. It would work with modest electric fields of <200 kV/m, and come at a reasonable cost.

12 Positron Sources and Positron Science

Table 5 presents parameters of positron sources and their electron-beam drivers for major past and present electron-positron colliders. Table 6 highlights the future needs. Figure 23 illustrates two big steps from SLC and SuperKEKB. The ILC e^+ source aims at four times the capture efficiency of SuperKEKB and 3 times the beam power of the SLC (74 kW). With its current design, based on an adiabatic matching device made of HTS, the FCC-ee source foresees 9 times the SuperKEKB capture efficiency, at a lower primary electron beam power (5-6 kW).

Table 5: Positron source parameters for past (SLC, LIL, CESR, VEPP-5, DCI) and present colliders (SuperKEKB, DAFNE, BEPCII) [from the presentation of I. Chaikovska]

Facility	**SLC**	**SuperKEKB**	**DAFNE**	**BEPCII**	**LIL**	**CESR**	**VEPP-5**	**DCI**
Research center	**SLAC**	**KEK**	**LNF**	**IHEP**	**CERN**	**Cornell**	**BINP**	**LAL**
Repetition frequency, Hz	120	50	50	50	100	60	50	50
Primary beam energy, GeV	30–33	3.5	0.19	0.21	0.2	0.15	0.27	1
Number of e^- per bunch	5×10^{10}	6.25×10^{10}	$\sim1\times10^{10}$	5.4×10^{9}	2×10^{11}	3×10^{10}	2×10^{10}	–
Number of e^- bunches /pulse	1	2	1	1	1	7-21	1	1
Incident e^- beam size, mm	0.6	~0.5	1	1.5	~0.5	2	~0.7	–
Target material	W-26Re	W	W-26Re	W	W	W	Ta	W
Target motion	Moving	Fixed	Fixed	Fixed	Fixed	Fixed	Fixed	Fixed
Target thickness/size, mm	20, r=32	14, r=2	-	8, r=5	7, r= 8	7, r=10	12, r=(~ 10–>2.5)	10.5, r= –
Matching device	AMD (FC)	AMD (FC)	AMD (FC)	AMD (FC)	QWT	QWT	AMD (FC)	AMD (Sol.)
Matching device field, T	5.5	3.5	5	4.5	0.83	0.95	8.5 (10 max.)	1.25
Field in solenoid, T	0.5	0.4	0.5	0.5	0.36	0.24	0.5	0.18
Capture section RF band	S-band	S-band	S-band	S-band	S-band	S-band	S-band	S-band
e^+ yield, N_{e^+}/N_{e^-}	0.8-1.2 (@DR)	0.4 (@DR)	0.012(@LE)	0.015(@LE)	0.006 (@DR)	0.002(@LE)	~0.014 (@DR)	0.02 (@LE)
e^+ yield, $N_{e^+}f(N_{e^-}E)$ 1/GeV	0.036	0.114	0.063	0.073	0.030	0.013	0.05 (@DR)	0.02 (@LE)
Positron flux,* e^+/s	$\sim6\times10^{12}$	2.5×10^{12}	$\sim1\times10^{10}$	4.1×10^{9}	1.2×10^{11}	7.6×10^{10}	1.4×10^{10}	–
Damping Ring energy, GeV	1.19	1.1	0.510	No	0.5	No	0.51	No
DR energy acceptance $\frac{\Delta E}{E}$, %	±1	±1.5	±1.5	No	±1	No	±1.2	No

Table 6: Positron source parameters for proposed future colliders [from the talk of I. Chaikovska].

Project	CLIC	ILC	LHeC (pulsed)	LEMMA	CEPC	FCC-ee
Final e^+ energy [GeV]	190	125	140	45	45	45.6
Primary e^- energy [GeV]	5	128** (3*)	10	–	4	6 →2.86 GeV
Number of bunches per pulse	352	1312 (66*)	10^5	1000	2	2
Required charge [10^{10} e^+/bunch]	0.4	3	0.18	50	1.88	~3.5
Horizontal emittance $\gamma\epsilon_x$ [μm]	0.9	5	100	–	16	24
Vertical emittance $\gamma\epsilon_y$ [μm]	0.03	0.035	100	–	0.14	0.09
Repetition rate [Hz]	50	5 (300*)	10	20	100	200 →100 Hz
e^+ flux [10^{14} e^+/second]	1	2	18	10–100	0.04	~0.1
Polarization	No/Yes***	Yes/(No*)	Yes	No	No	No

* The parameters are given for the electron-driven positron source being under consideration.
** Electron beam energy at the end of the main electron linac taking into account the looses in the undulator.
*** Polarization is considered as an upgrade option.

Crystal based/enhanced e^+ source was/is being tested at KEK and for FCC-ee. At the PSI SwissFEL proof-of-principle beam tests of an HTS-based e+ source with an HTS solenoid field of 12-15 T (prototype tested up to 18 T) as adiabatic matching device – see Fig. 24 – are planned to validate the innovative baseline solution for the FCC-ee (N. Vallis et al., PRAB 27, 013401 (2024)). In Japan, the full-scale prototyping of a non-baseline e- driven e^+ source for the ILC (Fig. 25) will be completed by 2027. This ILC source uses a conventional source S-band linac with much higher beam power.

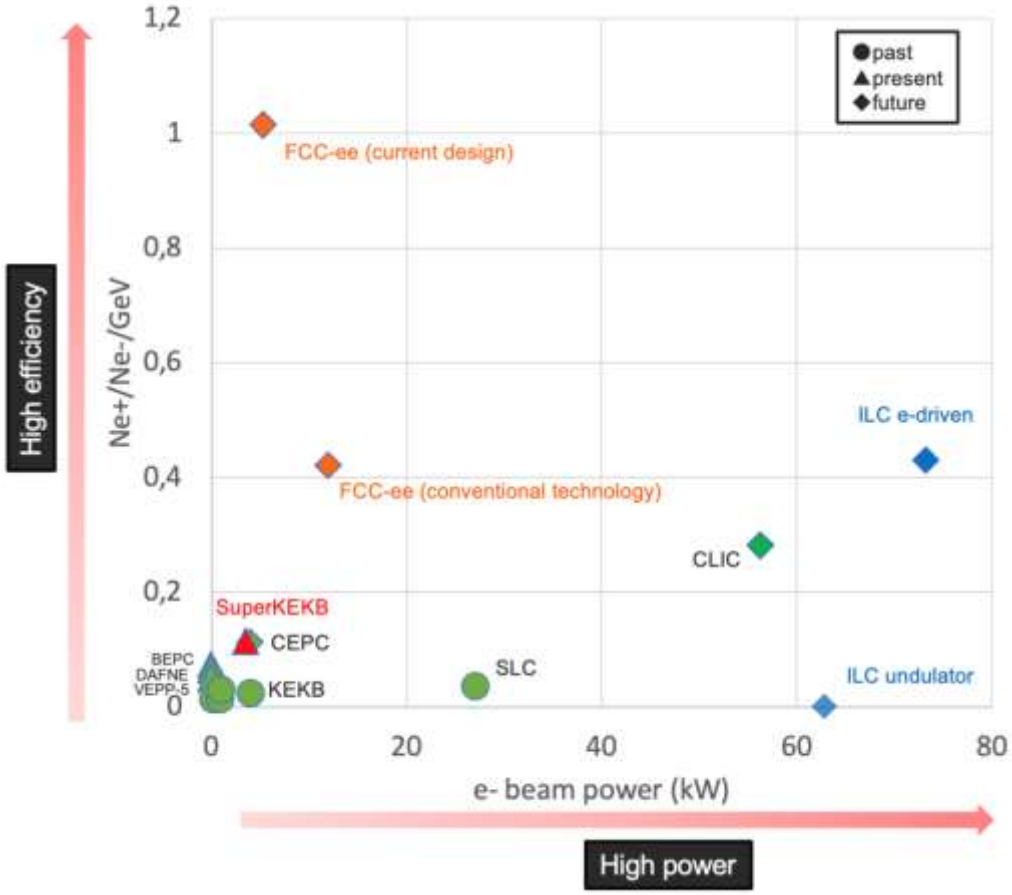

Figure 23: Past, present and future positron source efficiency (positron yield per primary electron per GeV electron energy) versus electron-beam power [from the presentation of I. Chaikovska].

Figure 24: The FCC-ee PoP e+ source at PSI (P3) with HTS solenoid as adiabatic capture device [from the presentation of I. Chaikovska].

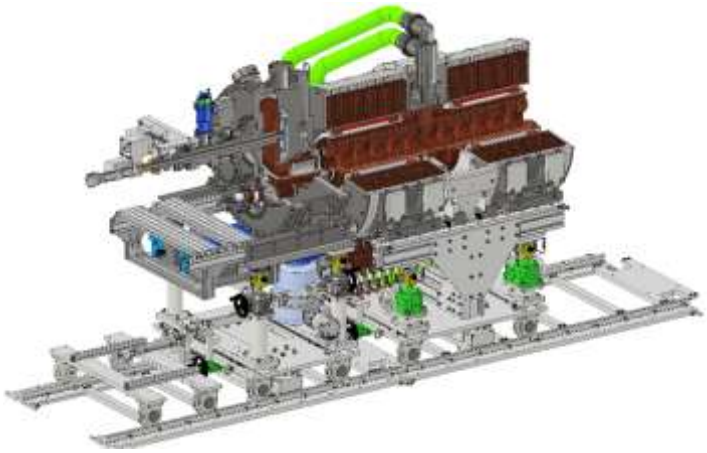

Figure 25: The non-baseline e^- driven ILC e^+ source based on a flux concentrator [from the presentation of I. Chaikovska].

13 Photon Sources including THz Sources

Figure 26 illustrates that much of our knowledge about proteins comes from accelerator based light sources ("X-Ray Diffraction"). The same is true for many other biological structures and inorganic materials. A key figure of merit for comparing different light sources is the brightness, defined as

$$\mathcal{B} = \frac{\dot{N}_\gamma}{4\pi^2 \sigma_x \sigma_y \sigma_{x'} \sigma_{y'} (0.1\%\mathrm{BW})}$$

with $\dot{N}_\gamma$ denoting the rate of photons per second, and the sigmas in the denominator the transverse rms photon beam sizes and divergences. After subtracting the correlations, this definition is independent of the distance to the source. Figure 27 reveals steep increases in the photon brightness due to the advent and further advances of accelerator-based slight sources, from the first storage rings, to linac-based free electron lasers (FELs).

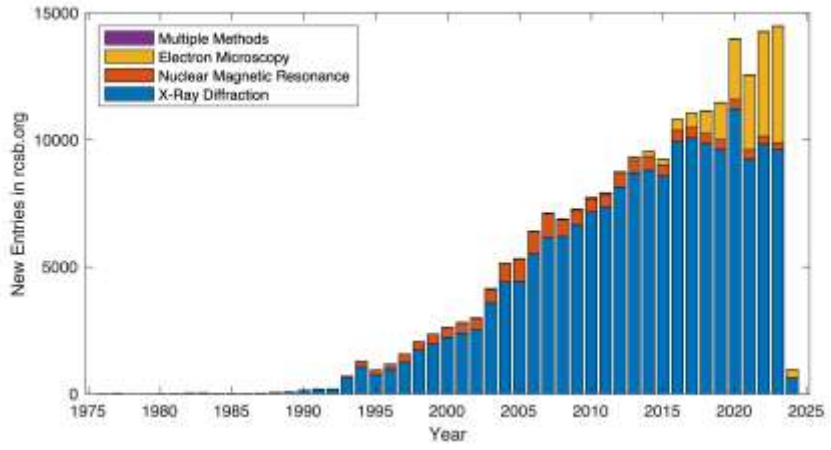

Figure 26: New entries in the RCSB Protein Database and from where the originated [from the presentation of R. Ischebeck].

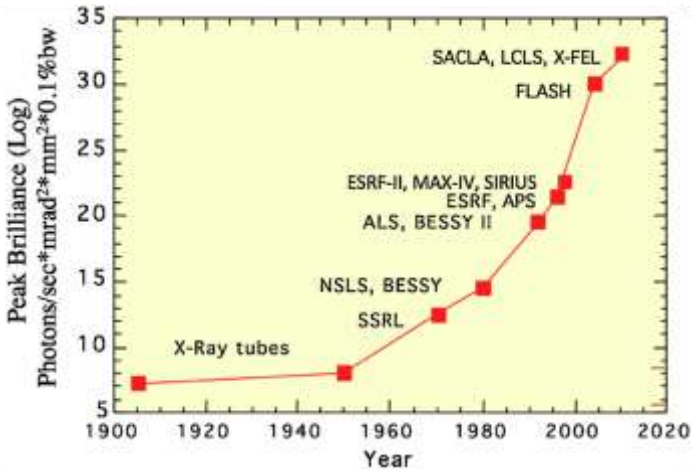

Figure 27: Increased of light source brightness over more than a century [from the presentation of R, Ischebeck].

Multibend achromat lattices yield much smaller horizontal emittances than a simple FODO lattice. ESRF and APS have already been upgraded based on this new lattice concept. The upgrade of SLS is underway (see Fig. 28). The horizontal emittance of the SLS will be reduced from 5630 pm at 2.4 GeV to 158 pm at 2.7 GeV.

Figure 28: Installation of magnets for upgrading Swiss Light Source SLS to SLS 2.0 [from the presentation of R. Ischebeck].

For FELs the "slice energy spread" is important. In case of the SwissFEL simulations with the code ASTRA predicted a slice energy spread of less than 1 keV, whereas measured values are 6.5 ± 0.5 keV at charge of 10 pC and 15.0 ± 0.3 keV at 200 pC. The larger energy spread in the real machine can be (at least partially) explained by intrabeam scattering and microbunching instability.

In China the HEPS 4th generation light source is under commissioning. Table 7 compares its parameters with other operating latest-generation machines. The beam commissioning through

establishing beam circulation and storing the beam was comparable, and slightly faster, than for a similar contemporary ring; see Fig. 29.

Table 7: Design parameters of several operating 4th generation light sources [from the presentation of Y. Yuan].

	HEPS	APS-U	ESRF-EBS	MAX-IV	Sirius
E(GeV)	6	6	6	3	3
C(m)	1360.4	1104	844.4	528	518
Lattice	7BA	7BA	7BA	7BA	5BA
Cell	48	40	32	20	20
Emittance (pm rad)	34	42	150	330	250
Brightness	$>10^{22}$	$>10^{22}$	$>10^{22}$	$\sim10^{21}$	$\sim10^{21}$
Construction period	2019~2025	2018-2024	2015-2020	2010-2016	2015-2018

Figure 29: HEPS beam commissioning compared with commissioning of another similar light source [from the presentation of Y. Yuan].

In Germany, the PETRA IV project considers replacing the existing PETRA III ring with an ultra-low emittance ring, adding a new Experimental Hall in two more octants, and replacing DESY II with a new low emittance booster. Figure 30 illustrates the general trend and the extreme performance expected from PETRA IV. PETRA IV will achieve an emittance of 20 pm at 6 GeV. It is foreseen to inject into PETRA IV from a 6 GeV laser plasma accelerator (see above). The time line of PETRA IV (Fig. 31) hinges on the project approval by mid 2026.

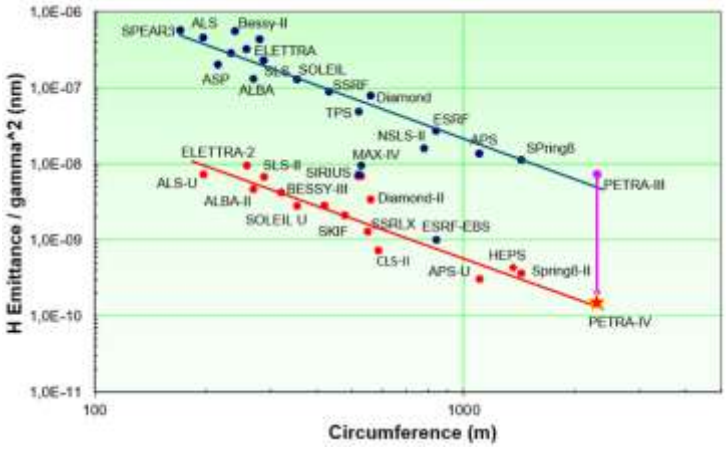

Figure 30: Landscape of low emittance ring. Energy-independent emittance factor versus ring circumference for past, present and future synchrotron light sources. The step from the blue to the red line was enabled by the transition from DPA/TBA cells to more extreme multibend achromat lattices [from the presentation of R. Bartolini and I. Agapov].

Figure 31: Time line of PETRA IV [from the presentation of I. Agapov and R. Bartolini].

Similar to SLS/SLS 2.0 and SwissFEL at Villigen, or PETRA-III/IV and the EuXFEL in Hamurg, also SPring-8 and SACLA in Japan are a light source storage ring and an FEL located on the same site. Figure 32 depicts the alternating long-term upgrade plan for these two facilities. The energy-efficient high-repetition rate SACLA-II FEL will ultimately be complemented by a coherent run source, SPring-8-III.

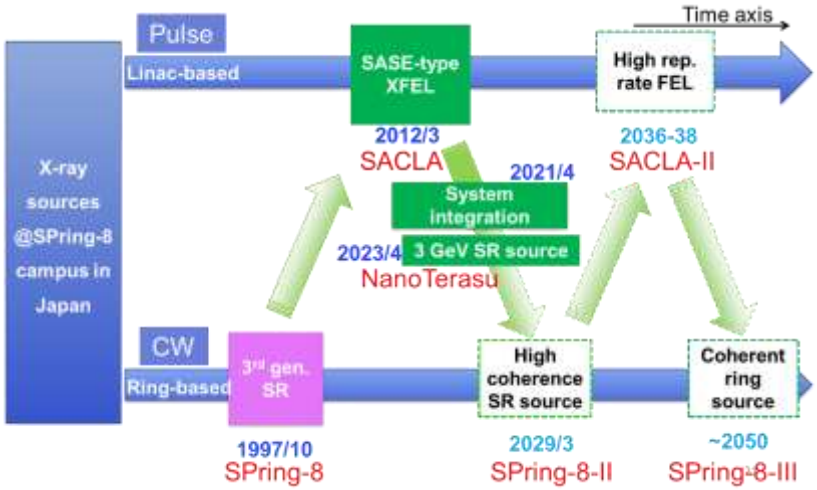

Figure 32: Long-term upgrade schedule for the SPring-8/SACLA facility [from the presentation of H. Tanaka].

Synergetic use of the FCC-ee booster ring as light source, will provide the ultimate source of photons with energies between ~50 and 150 keV. Figure 33 compares its estimate average and [peak brightness with other existing and proposed facilities. The synchrotron radiation from the FCC-ee booster could be fully transversely coherent down to wavelengths of 0.1 Å.

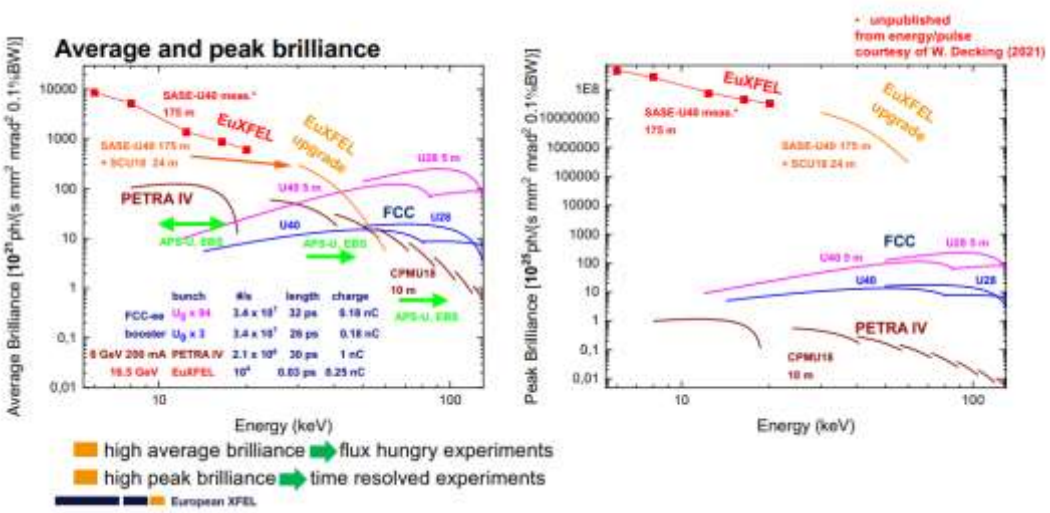

Figure 33: Average (left) and peak brightness (right) as a function of photon energy. The light purpose curves represent the FCC-ee booster, at 20 GeV injection energy, with a 28-mmm period undulator, the blue curve with a 40- mm undulators. The two different segments refer to different numbers of wigglers installed in the booster for additional emittance reduction [S. Casalbuoni, F. Zimmermann].

High gradient radio-frequency cryogenic copper structures with surface electric fields between 250 and 500 MV m^{-1} are enabling a new generation of photoinjectors with six-dimensional beam brightness beyond the current state-of-the-art by well over an order of magnitude. This advance is an essential ingredient for a novel ultra-compact XFEL developed at UCLA (UC-XFEL) [6]; see Fig. 34. Accelerating the low-emittance beam to GeV energies and then injected it into innovative, short-period (1–10 mm) undulators uniquely enable UC-XFELs having footprints consistent with university-scale laboratories, with expected photon production per pulse of a few percent of existing kilometre-scale XFEL sources.

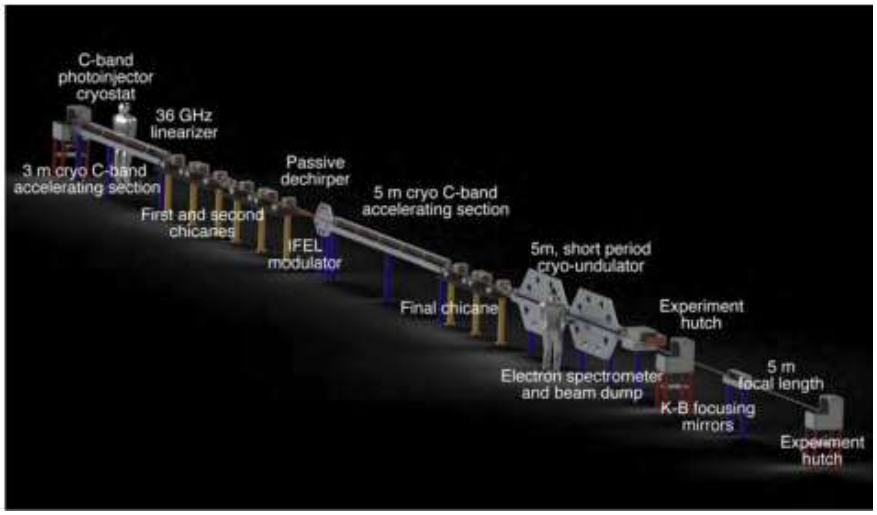

Figure 34: To-scale conceptual layout of the soft x-ray UC-XFEL, marking major component systems, with an end-to-end length of approximately 40 m. Human figures are shown for size comparison [6] [from the presentation of J. Rosenzweig].

To obtain hard (7 keV) X-rays, the UC-XFEL beam energy is increased to 2.44 GeV and the FEL design is extended to a regenerative amplifier (RAFEL) scheme based on a periodic train of electron pulses. This so-called XRAFEL, sketched in Fig. 35, greatly increases X-ray flux and coherence [7].

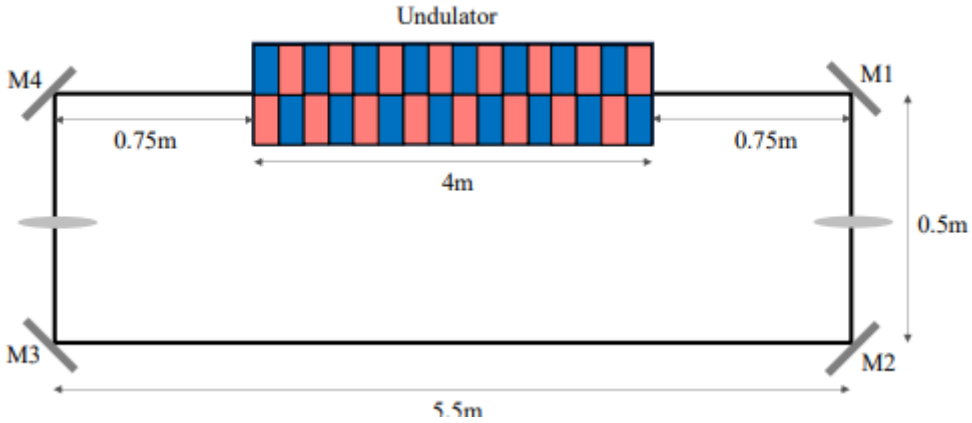

Figure 35: The setup of a 12 m round-trip cavity in an ultracompact XRAFEL. The radiation produced by lasing in the undulator is recirculated into the cavity and reflected via the Bragg condition [7] [from the presentation of J. Rosenzweig].

At KIT, the compact storage ring cSTART will be a superb THz radiation source, as shown in Fig.36. At cSTART, THz will be generated via coherent synchrotron radiation or undulator emission, in the form of ultrashort (few 100 fs) THz pulses at a high repetition rate with extreme electric fields, e.g. 3.3 GV/m at 10 Hz or 1.0 GV/m at 6 MHz, comparable to the much larger LCLS facility at SLAC. cSTART can also produce X-rays via inverse laser-driven inverse Compton scattering (Fig. 37).

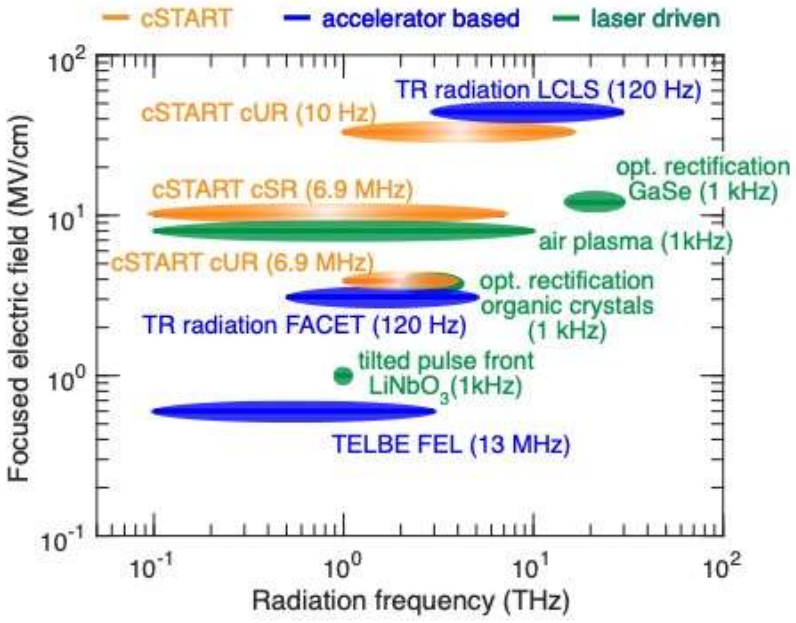

Figure 36: cSTART as ultrafast high-field THz radiation source [from the talk of M. Fuchs].

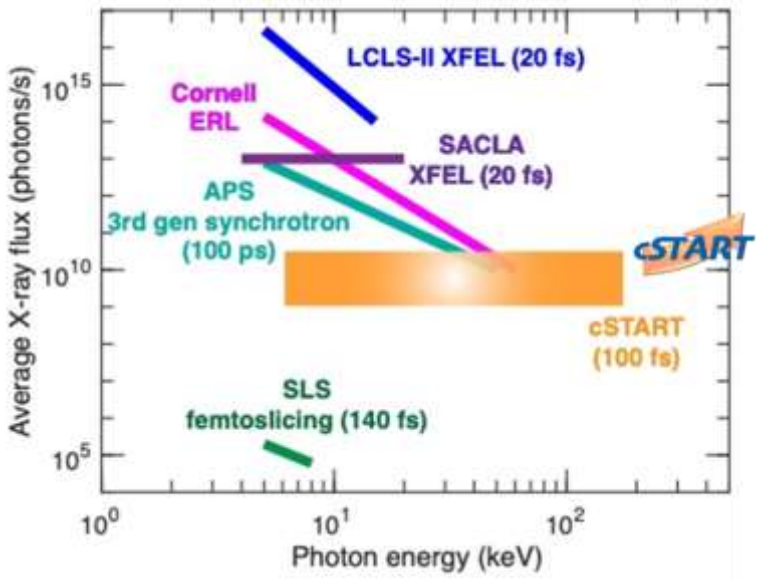

Figure 37: cSTART as source of ultrashort X-ray pulses with high average power [from the presentation of M. Fuchs].

Unlike single particles, quasiparticles, which are the result of collective motion, e.g., in a plasma, can be subject to arbitrary acceleration and travel at any velocity [8,9]. These quasiparticles may generate novel forms of radiation forbidden for single particles, such as quasiparticle Cherenkov superradiance, subluminal and superluminal quasiparticle undulator radiation. The frequency range accessible by a plasma accelerator-based photon source spans nearly 10 octaves, from THz to the extreme ultraviolet, as is illustrated in Fig. 38.

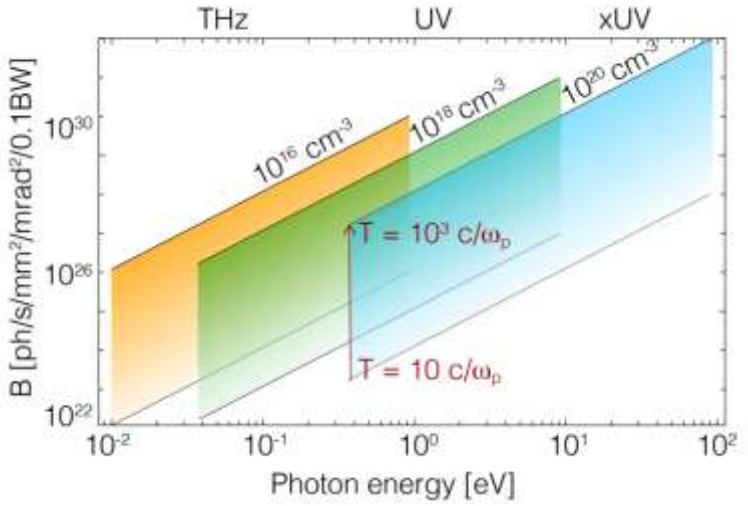

Figure 38: Photon beam brightness expected from plasma-based quasiparticle photon source as a function of photon energy [8,9] [from the presentation of J. Viera].

14 Neutron Sources

Neutron sources support several fruitful research fields, including new areas of research on energy protein structure, high strength alloys, polymer materials, and magnetic material. Neutrons can be produced in a number of ways, illustrated in Fig. 39. All of these processes may involve accelerators.

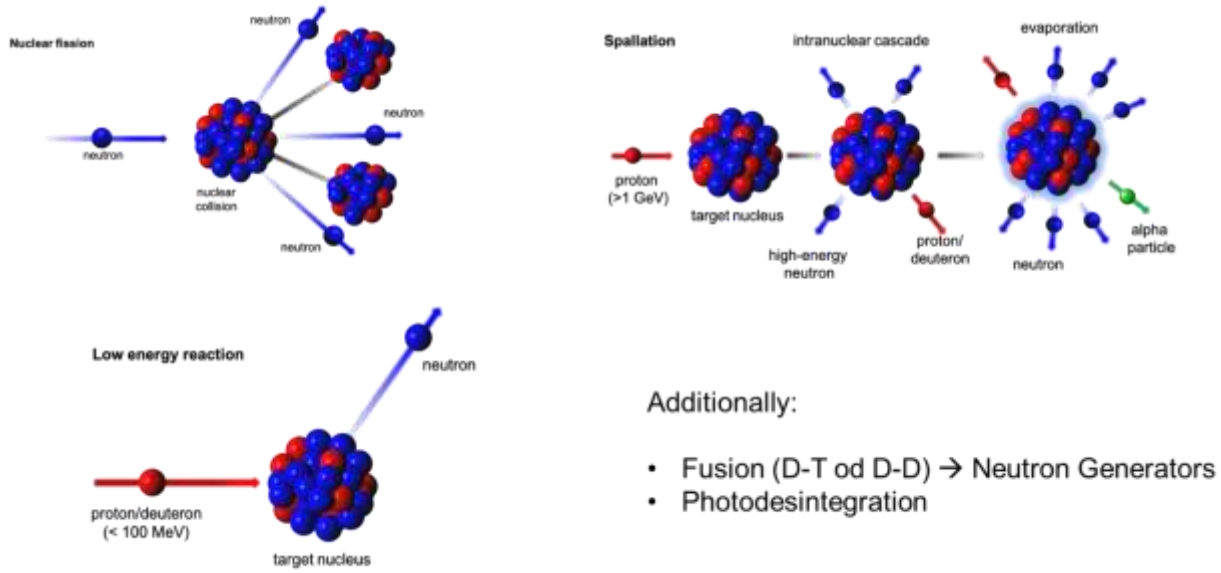

Figure 39: Production of free neutrons [from the presentation of H. Podlech].

The composition of users for the Chinese SNS (CSNS) is illustrated in Fig. 40. CSNS delivers a beam power of 140 kW, exceeding its design value. A power upgrade, CSNS-II, with 0.5 MW power has been approved, with an average beam current of 312 μA. Its key ingredient is a new SC linac; see Fig. 41.

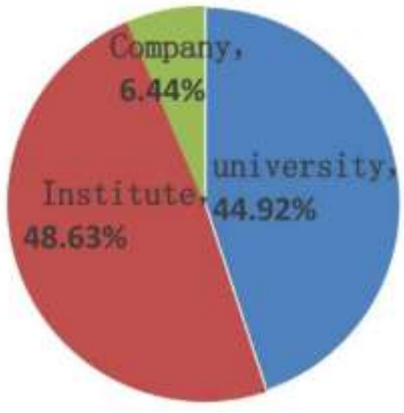

Figure 40: Distribution of SNS neutron users [from the presentation of Y. Yuan].

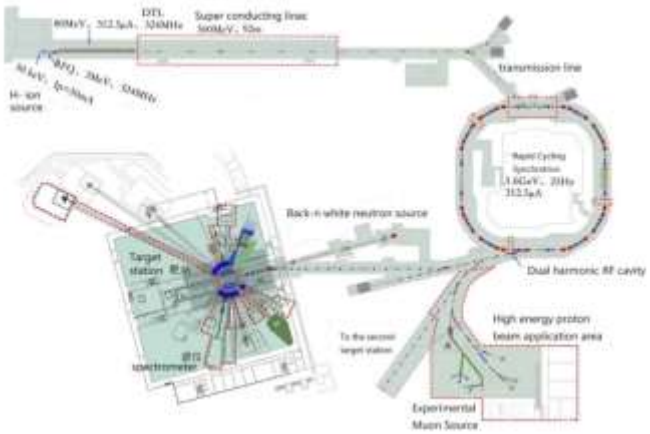

Figure 41: CSNS-II as an upgrade of CSNS-I [from the presentation of Y. Yuan].

Among other uses, the CiADS, soon to be completed, will send proton beams onto a high-power lead-bismuth eutectic (LBE) spallation target for neutron production.

In addition to the major large accelerator-based neutron sources, like SNS, ESS and CSNS, the shutting down of nuclear reactors in parts of Europe, calls for additional more compact neutron sources.

The LENS collaboration pushes proton-driven sources. The FRANZ neutron source is in an advanced construction state at GU Frankfurt; see Fig. 42. FRANZ will be paused at repetition rates up to 250 kHz (100 ns pulses), with a beam energy around 2 MeV and a beam current of 30 mA. First neutrons from FRANZ are expected in July 2025.

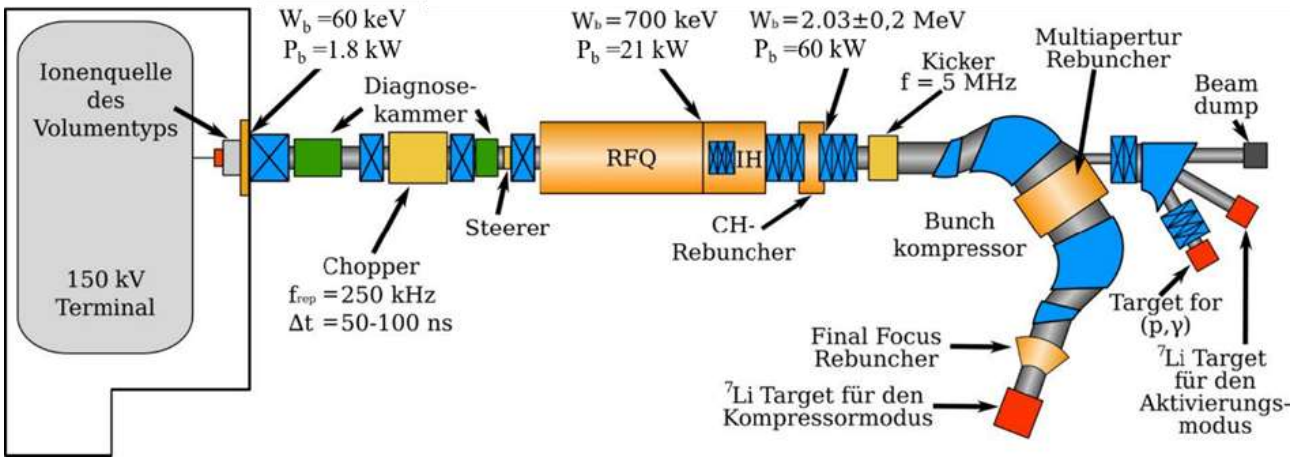

Figure 42: The rapidly pulsed neutron source FRANZ at IAP Frankfurt [from the presentation of H. Podlech].

A more brilliant source, High Brilliance Neutron Source (HBS) – see Fig. 43 –, developed at FZ Jülich, will be the flagship project for a new class of High Current Compact Accelerator-Based Neutron Sources (HiCANS), using low energy proton accelerators (< 100 MeV).

Figure 43: The HBS under development by FZ Jülich and Frankfurt's IAP [from the presentation of H. Podlech].

Figure 44 illustrates the location of HBS in the energy-beam current landscape of modern proton linacs.

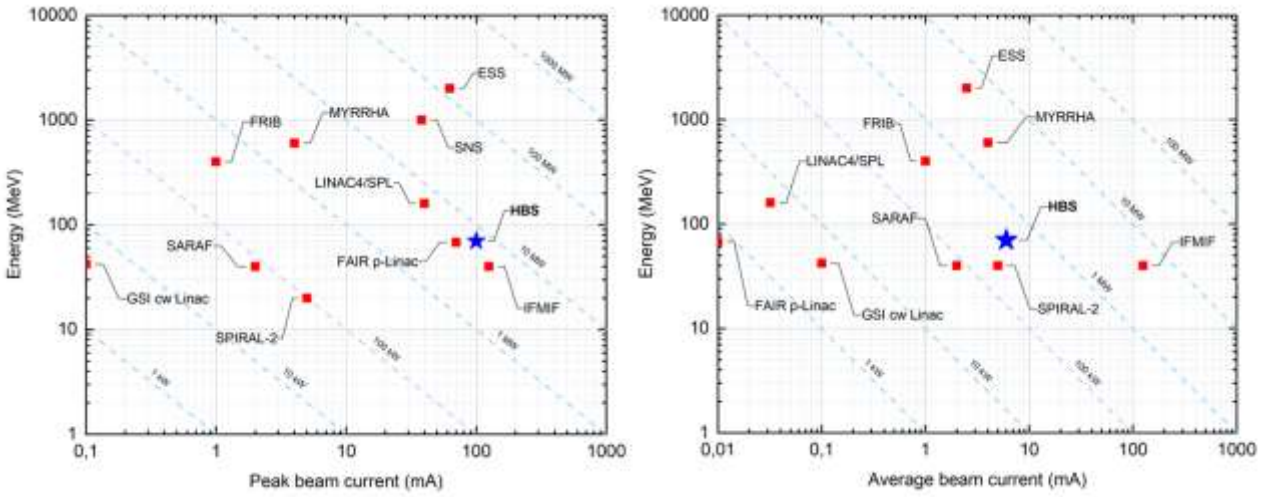

Figure 44: Energy versus peak (left) and average beam power (right) of modern hadron linacs. The blue star represents the future compact neutron source HBS [from the presentation of H. Podlech].

Recent efforts also comprise the completely different, novel concept of an electron beam driven neutron source. Here electrons are sent onto a target, e.g. made form tungsten, where they suffer from bremsstrahlung, which can excite giant dipole resonances, which then leads to neutron emission.

A figure of merit is the source strength, defined as the product electron current and yield. Figure 45 compares present and projected total source strengths for different types of neutron sources, indicating that, in terms of beam power efficiency, electron beam driven neutron sources are well competitive with those based on proton beams.

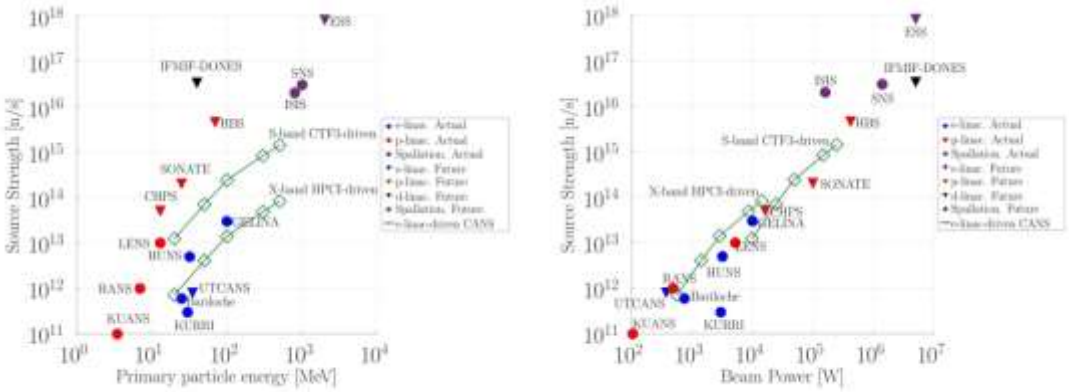

Figure 45: State of the art comparison of hadron-driven (red, black, and purple) and electron-driven neutron sources (blue and green), showing source strength (vertical axis) as a function of primary particle energy (left picture) and beam power (right picture) [from the talk of J. Olivares Herrador].

Moderating neutrons and extracting neutrons of different temperatures is an art in itself. The system for the electron-beam driven source e-CANS is not yet fully optimized. Figure 46 places its presently simulated performance into the landscape of average and peak brightness for thermal and cold neutrons.

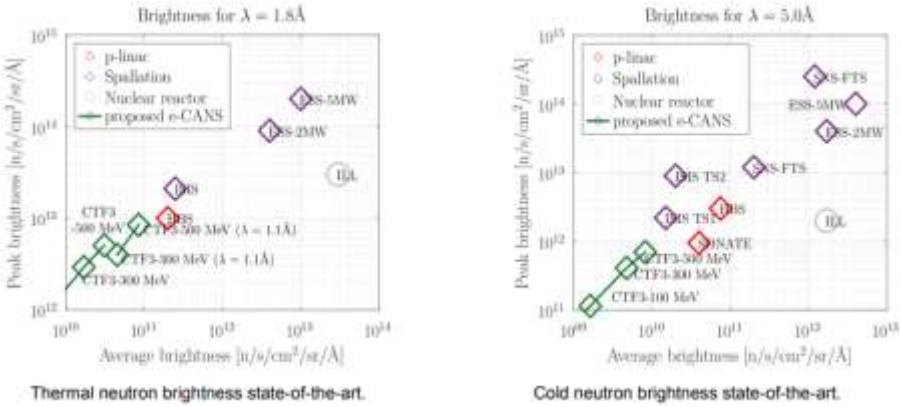

Figure 46: Different proposed, upcoming or existing neutron sources shown in the plane of peak brightness (vertical axis) versus average neutron brightness (horizontal axis) for thermal and cold neutrons (horizontal axis, right picture) [from the presentation of J. Olivares Herrador].

Another approach is the beam-chaser concept mentioned in Section 3. Figure 47 presents a schematic of a directional neutron source. A total directional neutron rate of order 6.25×10^{14}/ sec would be within reach.

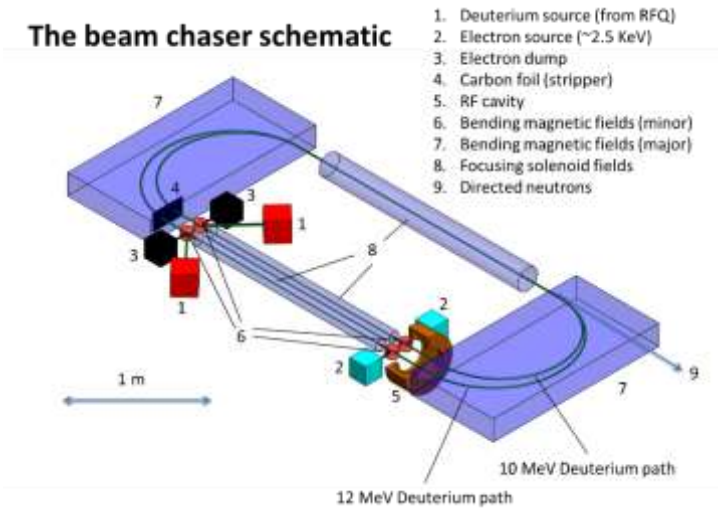

Figure 47: The "beam chaser" based directional neutron source – an all magnetic ring allowing rear-end collisions of different ions such as of 10 MeV deuterons with 12 MeV deuterons (as sketched) or of deuterons with tritons at rms spot sizes below 300 μm [2] [from a presentation of J. Rosenzweig].

15 Collisions in a co-moving frame

Particle kinetic energies of order 100 keV to 1 MeV are required to be comparable with Coulomb potential energy barrier heights [3]. To study spin dependence in nuclear scattering, one must make the scattering occur in a moving frame of reference. Such collisions could possibly be realized in the GSI ESR ring, as had been proposed by B. Franzke as early as 1967. Similar collisions in a magnetic "beam chaser" configuration (see Fig. 45) were proposed by J. Rosenzweig and the UCLA group.

Colliding different co-moving ion species is also possible in a predominantly electric storage ring with weak magnetic bending superimposed. Such an "E&m" storage ring can store two different particle type bunches, such as triton (t) and helion (h), h and deuteron (d), or h and electron (e^-), co-traveling with different velocities on the same central orbit. Figure 48 illustrates the possibility of stable buckets for beams of different velocity in such a ring. Figure 49 shows the lattice layout for a prototype E&m ring.

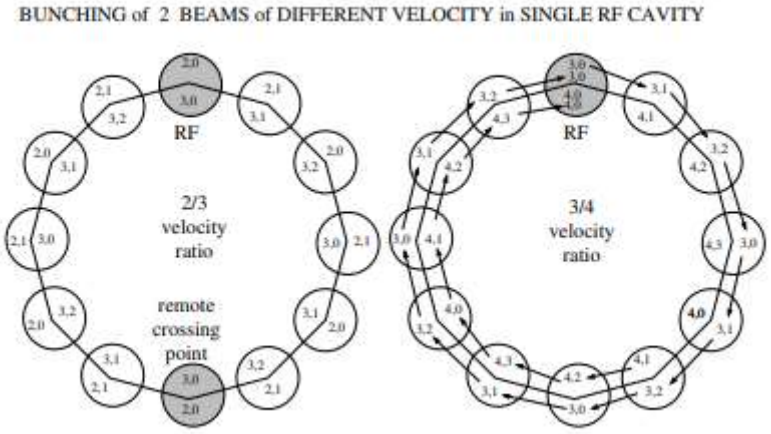

Figure 48: Stable RF buckets for different velocity ratio beams [4] [R. Talman].

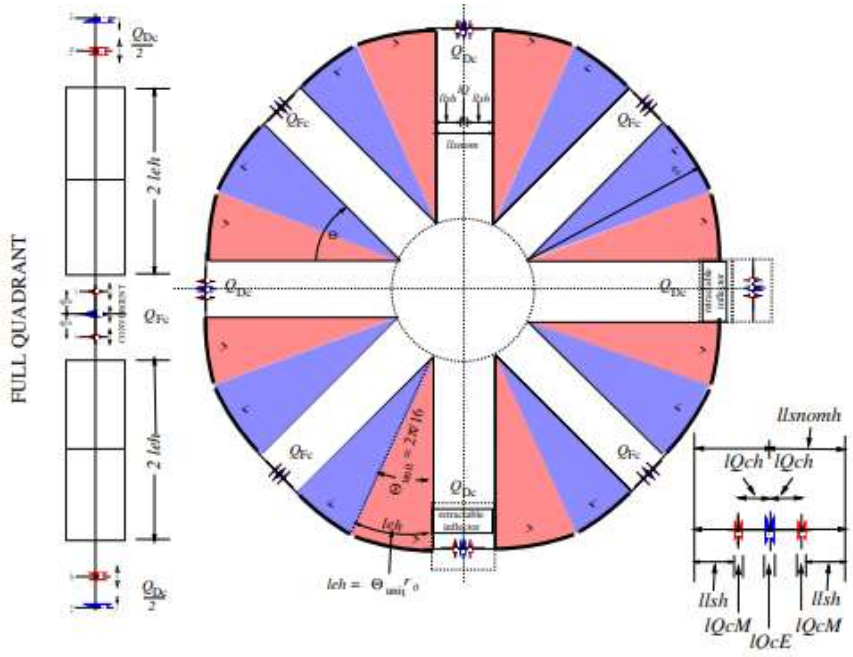

Figure 49: Lattice layouts for PTR, the proposed prototype nuclear transmutation storage ring prototype; "compromise" quadrupole lower right, where the magnetic quadrupoles are split into two portions placed on either side of the electrostatic quadrupole lenses. The circumference is chosen as 102 m, but the entire lattice can be scaled, e.g., to reduce peak field requirements [4] [R. Talman].

Rear-end collisions occurring periodically in a full acceptance particle detector/polarimeter, will allow the (so far inaccessible) direct measurement of the spin dependence of nuclear transmutation for center of mass (CM) kinetic energies (KE) ranging from hundreds of keV up toward pion production thresholds. By measuring the spin dependence of nuclear interactions around the Coulomb barrier, such a machine can provide experimental data to refine our understanding of the nuclear force and its influence on high energy physics. Increasing local particle density with a low-beta insertion also fusion reactions between tritons and deuterons could be generated, possibly helping to optimise

the design of future fusion reactors or even paving a way towards an accelerator based dual-species fusion energy source [5].

16 Compact high-precision storage rings

Recently several high-precision electric or electric-magnetic storage rings have been designed for a variety of nuclear physics and particle physics applications. These include the dual-species rear-end collider, discussed above. Other, prominent examples are the EDM rings to measure the electric dipole moments of charged particles such as protons; see Fig. 50. Many studies very relevant for proton EDM rings were executed at COSY using deuterons.

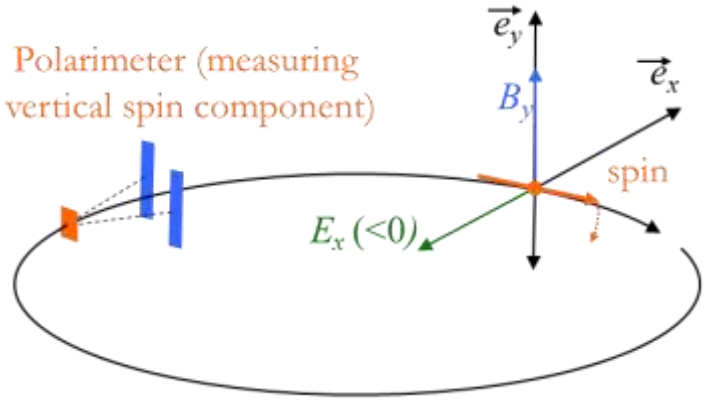

Figure 50: Sketch of a generic EDM ring [from the presentation of C. Carli].

A “frozen spin” is preferred for static EDM measurements, where a nonzero static EDM would induce a spin rotation out of the horizontal plane. The frozen spin with electric fields is possible only for particles with a positive anomalous magnetic moment factor by operation at an appropriate “magic” energy. Issues are spin (de-)coherence and systematic effects (e.g. vertical spin build-up with MDM only could be mistaken as EDM). Several of these systematic effects can be mitigated by operation with counter-rotating beams There are several variants, e.g. a hybrid ring with magnetic quadrupoles, as an alternative to the fully electro-static ring.

The community has agreed on a staged approach, which has started with the first direct cpEDM measurements on deuterons and many basic studies at COSY, and foresees as the next step a prototype ring to gain experience and better understand the limitations and their mitigations (see Fig. 51).

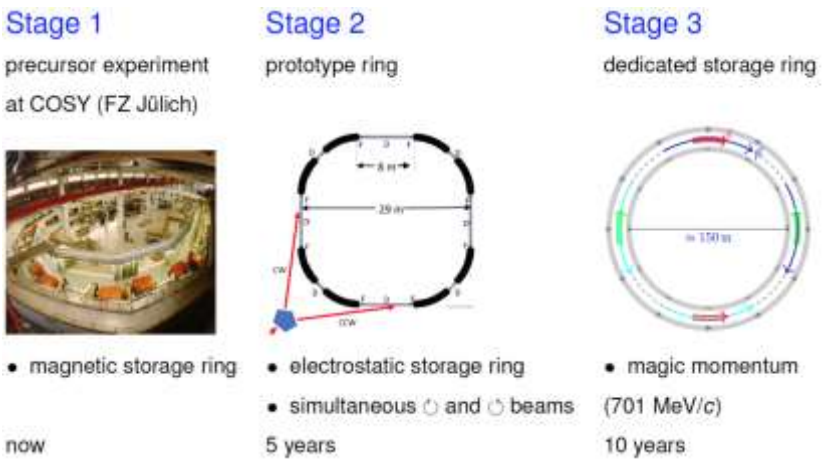

Figure 51: Staged approach to EDM measurements with the design of a prototype ring as the next step [from the presentation of C. Carli].

A future compact electron storage ring, already approved, is the "compact STorage ring for Accelerator Research and Technology" (cSTART), which will be constructed at KIT to study fundamental accelerator physics. Figure 52 shows an illustration. cSTART is designed with a large momentum acceptance (~4%), to store ultrashort electron bunches and to allow for direct injection of an ultrashort bunch from a laser plasma accelerator. cSTART is not only compact but also energy efficient, and it will allow for widely unexplored accelerator physics and technology developments, preparing for a new generation of future light sources with potential for transformative impact.

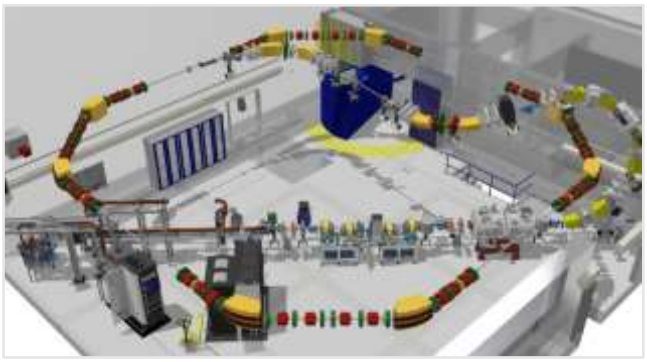

Figure 52: cSTART, with14 m diameter, producing ultrashort X-rays [from the talk of M. Fuchs].

17 Medical accelerators

About a third of the world's tens of thousands of accelerators serve for medical uses: imaging, radioisotope production, and cancer therapy.

Particle cancer therapy is based on the Bragg peak, with a highly localised dose distribution, but the steep dose gradient introduces a sensitivity to range uncertainties (inter-/intra-fractional anatomic changes, planning uncertainties, patient set-up, motion induced range variation). One solution is mixing carbon and helium ion beams (90% C, 5-20% He) with a similar mass-to-charge-ratio. The range of He ions through a patient's body is ~3 times larger than for C ions at the same

energy/nucleon. Carbon is used for irradiation, while helium passes patient for real-time online monitoring. The online range verification provides for an extraordinary increase in precision of the conformal dose delivered. The concept is illustrated in Fig. 53. First in the world, GSI is presently commissioning such a novel dual ion beam for cancer therapy.

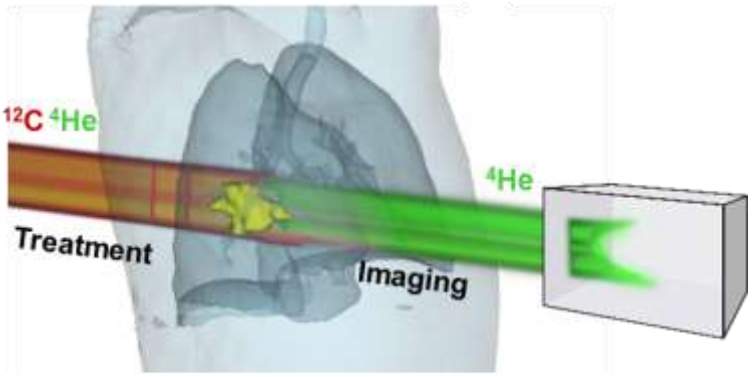

Figure 53: Dual-beam cancer therapy with carbon-ion radiation and helium-ion online monitoring, pioneered at GSI in Darmstadt (Ch. Graeff, L. Volz, M. Durante, Prog. Part. Nucl. Phys., vol. 131, 104046, Jul. 2023) [from the presentation of R. Assmann].

Another promising approach to accelerator-based cancer therapy its Boron-Neutron Capture Therapy (BNCT), based on the reaction $n+^{10}B \rightarrow {}^{7}Li + \alpha$, with a high cross section. The isotope ^{10}B is brought exclusively to tumour cells. BNCT requires proton linacs with an energy 5-10 MeV, an average beam current of 10-20 mA, and average beam power 100-200 kW. Figure 54 shows a commercial BNCT that should soon be available.

Figure 54: A BNCT linac developed by Bevatech, FZ Jülich and IAP Frankfurt [from the presentation of H. Podlech].

18 Compact advanced injectors

Laser target normal sheath acceleration (TNSA) of ions allows for much more compact hadron accelerators. The LIGHT collaboration centered at GSI is improving laser ion generation, handling and transport so as to enable user operation. Figure 55 depicts the front part of the LIGHT beam line, also indicating beam parameters at different stages. Connecting this beam line to the GSI complex allows for a proof of principle demonstration of a TNSA laser-ion injector. This concept could reduce injection time, the ion beam emittance / bunch length, as well as the cost and size of future hadron injectors. Immediate benefits for GSI include the expansion of the variety of ion species that can be injected, and securing a spare injector – Fig. 56.

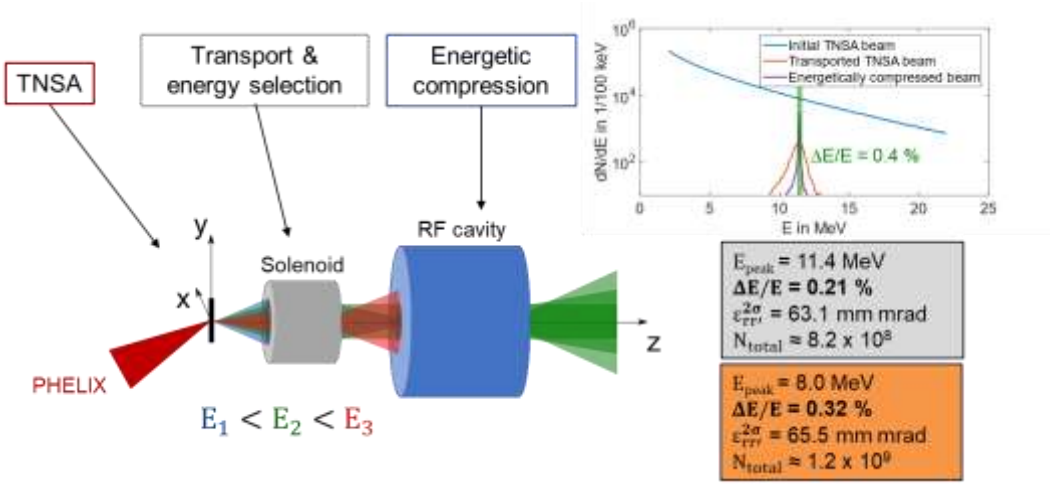

Figure 55: Schematic of the GSI LIGHT beam line front end [from the talk of R. Assmann].

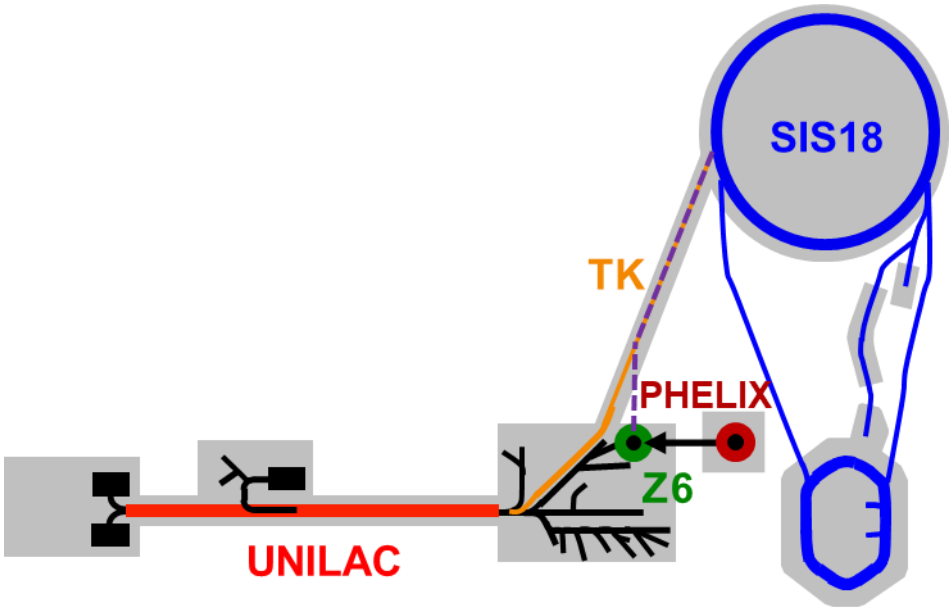

Figure 56: HELIX-Z6 LIGHT beam line as advanced injector for the GSI complex [from the presentation of R. Assmann].

For electron beams, PETRA IV plans to replace a conventional injector by a compact laser-plasma injector as a sustainable alternative to a more conventional injector chain consisting of the existing LINAC II and the DESY IV synchrotron; see Fig. 57. The next 3 years will be focused on the demonstration of high-quality beam suitable for high efficiency injection in PETRA IV and high reliability of the injector

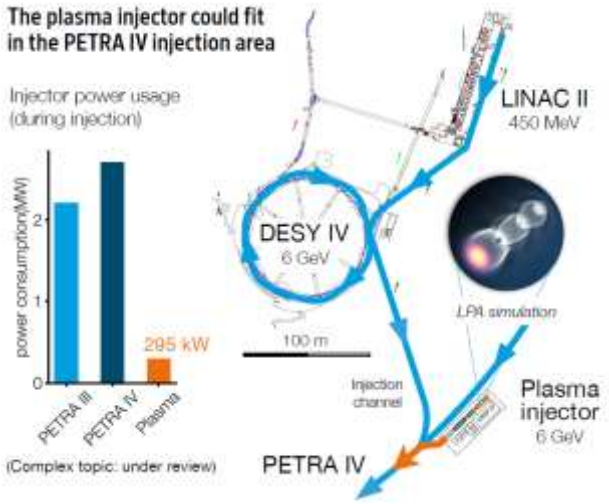

Figure 57: Alternative injectors into PETRA IV, namely Linac II and DESY IV, or a plasma accelerator (right) and comparison of injector power usage (left) [from the presentation of R. Bartolini and I. Agapov].

LPA injectors will also be studied at cSTART in different ring/LPA operating regimes, particularly for injecting ultrashort bunches (few – tens of fs); see Fig. 58.

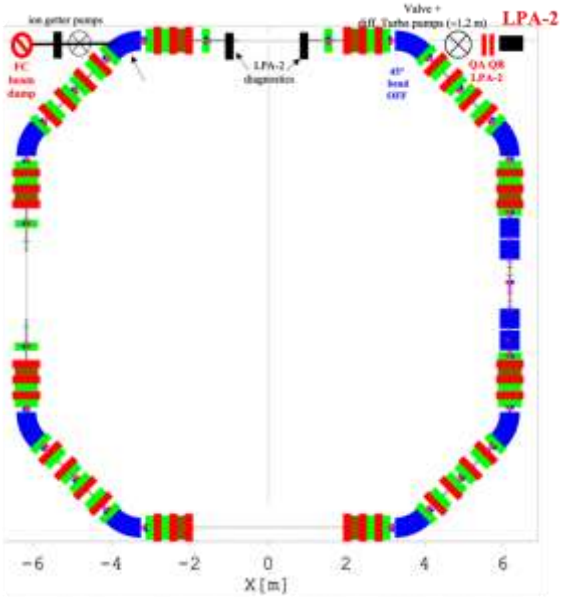

Figure 58: cSTART with LPA injector [from the presentation of M. Fuchs].

19 Nano-Accelerators

Far exceeding gradients inside plasma accelerators, in principle, both crystals and carbon nanotubes (CNTs) can support acceleration levels of 100s of TeV/m. Surface plasmons are excited by either charged particle beams or photon beams, allowing to produce PeV electrons on the meter length scale. Figure 59 illustrates different regimes of CNT acceleration, observed in simulations considering charged particle beams as driver [10]. Proof-of-principle experiments are proposed and planned at various facilities, for example beam-driven experiments at CLARA in the UK and FACET-II in the US, and a laser-driven experiment at the Pulsed Laser Center (CLPU) in Salamanca, Spain.

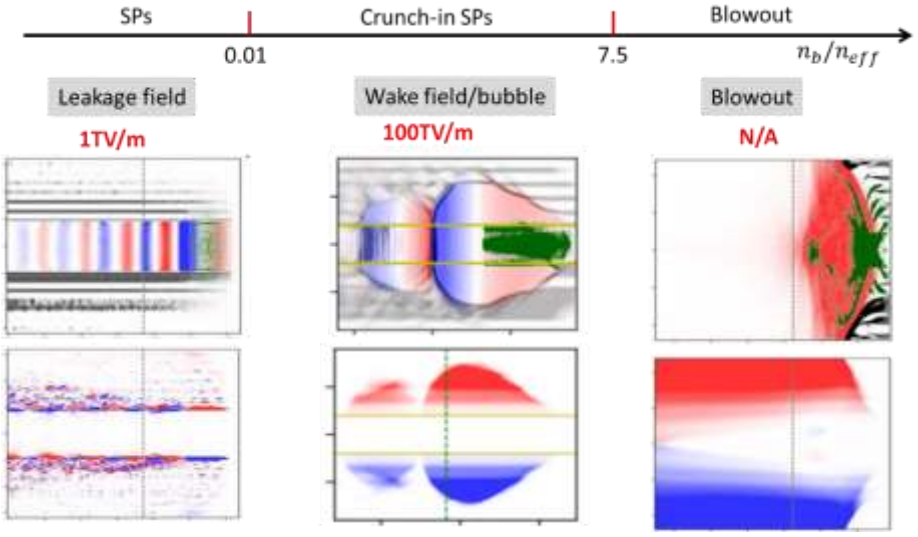

Figure 59: Different regimes of CNT acceleration include surface plasmons with leakage fields, and surface plasmon crunch-in. Only the CNT "blow-out" regime on the right is not suitable for particle acceleration [10].

20 Conclusions and Recommendations

The accelerator landscape is rapidly evolving. Accelerators can play an important role in solving societal problems. Key findings are summarized as follows:

- Accelerators can help produce ***safe and efficient electrical energy***, e.g., in ***accelerator-driven systems*** or as enablers of ***nuclear fusion.***
- ***Spin-transparent storage rings*** can become the ***ultimate quantum computers***.
- Accelerators will provide ***better, more efficient, more intense and more compact sources of photons, neutrons, and positrons*** for a plethora of applications and large user communities.
- Accelerators advance and revolutionize efficient ***cancer therapy***.
- ***Novel accelerator-based neutron sources*** include compact proton-beam based sources like HBS in Germany and electron-beam driven neutron sources, such as those based on CLIC or FCC-ee type linear electron accelerators. These can replace nuclear reactor-based sources and also allow for a more widespread availability of neutron-based research.
- Tantalizing new concepts such as ***quasiparticle radiation*** and ***nano-accelerators*** may prove transformative.
- ***Crystalline beams*** are celebrating a comeback in Europe.
- ***Compact storage rings and beam chasers*** are opening up a window to hitherto impossible experiments in nuclear and particle physics, which could help uncover physics beyond the Standard Model and new insights into nuclear physics.
- Accelerators are getting ever more ***energy efficient.***
- ***Machine learning and advanced manufacturing processes*** will boost accelerator performance and lower their cost.

The past 3.5 years of iFAST activities have catalyzed the ongoing R&D in the accelerator community. Following its mandate, iFAST Task 5.2 created a framework for exchanging experiences and ideas. The set of iFAST events and discussions did not allow for drawing a unique roadmap. In this report, we could, however, identify several distinct areas in which accelerator science and technology are developing or where new concepts are emerging. Table 8 summarizes the situation and lists some key recommendations as an outcome of iFAST Task 5.2 Pushing Accelerator Frontiers. Specific conclusions and recommendations formulated at the roadmap workshop are compiled in Annex A.

Table 8: Summary, perceived status, and recommendations by topical area

Area	Sub-area	Status	Roadmap status and goal	Impact	Recommendation
Sustainability	MORE SUSTAINABLE AND MORE EFFICIENT ACCELERATORS	Under development	Future goal and focus	High	This area should be vigorously expanded. IFAST has provided an initial framework, and identified key R&D needs to be addressed.
	ACCELERATORS SOLVING THE ENERGY PROBLEM	Conceptual	Future goal and focus	Very high	
High Energy	FUTURE COLLIDERS	Feasibility studies up to global engineering designs	Near future approval	Very high for particles physics, likely spinoffs for society	This sector is well developed. The technological aspects for HTS magnets are of strategic interest with great benefit in numerous areas.
	HIGHER-FIELD ACCELERATOR MAGNETS	R&D program	Industrialization	High Societal	
	HIGHER POWER HADRON MACHINES	Under construction & proposed upgrades	Advancement with spinoffs	High for nuclear physics, with great synergies	This sector is already advancing thanks to several important flagship programs (J-PARC, PIP-II/III, HIAF, FAIR, SNS, ESS, CSNS...)
	FASTER ACCELERATOR CONSTRUCTION	Efforts for FAIR, MYRRHA and HIAF	Ongoing and Goal	Speed-up	Growth area with potentially great benefits in the future in terms of time, cost, and performance.
AI & Accelerators	ACCELERATOR AI: BETTER DESIGN, OPERATION & PHYSICS	Worldwide efforts	Coupled to AI development	Potentially high	Fast development of AI applications should be followed and exploited. AI tools can help improve accelerator operations and design.
Synergies	SYNERGETIC AND COMBINED ACCELERATOR APPLICATIONS	Exploratory	Expanding	High if combined	This concept gains importance (examples SPring-8/SACLA, FCC). Maximizing the use of resources and return on investment, while minimizing power consumption.
(Re-)Emerging fields	CRYSTALLINE BEAMS	Reviving	Planned	Not evaluated	This area is to be expanded to realized novel types of beams and important new uses of accelerators.
	STORAGE RINGS FOR QUANTUM COMPUTING	Conceptual	Goal	Potentially high	
Novel sources	FUTURE POSITRON SOURCES AND POSITRON SCIENCE	Ongoing R&D	Near future	High	The development of sources is ongoing, but the quest for more efficient and better-quality sources is fundamental. Novel sources will have a transformational impact on various areas of science.
	FUTURE PHOTON SOURCES INCLUDING TH2 RADIATION	Proposed and under construction	Near goal	High	
	NEUTRON SOURCES	Novel concepts	Planned demonstration	High	
Advanced Beams & accelerators	COLLISIONS IN A CO-MOVING FRAME	Re-discussed	Future	Novel	This is an exciting pathway for accelerators and beams. Approaches, step-wise implementation and challenges to be explored.
	COMPACT HIGH-PRECISION STORAGE RINGS	Frozen	Future	Very high	
Health & accelerators	MEDICAL ACCELERATORS	Fast developing	Near goal	High	Many accelerators for medical application already exist. A next generation of facilities will use FLASH therapy or dual-species treatment.
Future concepts	COMPACT ADVANCED INJECTORS	R&D	Future goal	Potentially high to very high	Exploratory studies should assess critical bottlenecks and develop mitigation measures or scheme modifications.
	NANO-ACCELERATORS	Conceptual, R&D	Future goal	Potentially very high	

References

[1] iFAST WP5.2 joint Brainstoring & Stargey workshop on the Roadmap for Future Accelerators (iBiF 2024), Frankfurt a.M, Germany, 1-3 September 2024

[2] J. Rosenzweig, "New ideas for fusion/neutrons: pulsed and beam-based approaches," CERN ABP Forum, 18 November 2014.

[3] R. Talman, "Neutrino mass measurement background suppression using a predominantly electric E@m storage ring," ICFA mini workshop: Beam-Beam Effects in Circular Colliders (BB24), EPFL, Lausanne, 2-4 September 2024.

[4] R. Talman, "Predominantly Electric Storage Ring E&m for Nuclear Spin Physics," Proc. SPIN 2023

[5] R. Talman, "Neutron-free, deuteron/helium3 Thermonuclear Power Development at COSY," FZ Jülich, 5 October 2022

[6] J.B. Rosenzweig et al., "An ultra-compact x-ray free-electron laser," New J. Phys. 22 093067 (2020)

[7] J.B. Rosenzweig et al., "A High-Flux Compact X-ray Free-Electron Laser for Next-Generation Chip Metrology Needs," Instruments 2024, 8, 19. https://doi.org/10.3390/ instruments8010019.

[8] J. Viera, "Superradiant XUV emission from plasma accelerator based light sources, " at 2nd Workshop on Applications of Nanostructures in the field of Accelerator Physics, Parc Científic - University of Valencia, Valencia, Spain, Sep 17 – 18, 2024,

[9] B. Malaca et al., "Coherence and superradiance from a plasma-based quasiparticle accelerator," arXiv:2301.11082.

[10] B. Lei, "Simulation of beam-driven carbon nanotube-based electron and positron acceleration," at 2nd Workshop on Applications of Nanostructures in the field of Accelerator Physics, Parc Científic - University of Valencia, Valencia, Spain, Sep 17 – 18, 2024,

Annex A: Conclusions from iBiF2024 discussion

The conclusions discussed at the end of the iFAST workshop iBiF2024 at Goethe University Frankfurt resulted in the classification, shown below, according to three main (alternative) criteria: 1) Facilities; 2) Technology & Physics development; 3) Megatrends. This classification was the first step towards the more refined Table 8.

Facilities

1) More effort on ADS: MYRRHA, CiADS
2) For nuclear physics, the future is FAIR, HIAF, EIC, CNUF
3) For photon science big machine HEPS, Petra IV, Spring8 (2 and 3), SLS2, SACLA2, EuXFEL upgrade, SwissFEL2; using FCC_ee as hard X-Ray circular light source
4) For neutron science: more compact and novel approach, ESS, CSNS, SNS
5) For particle physics FCC is one option for Europe, but not approved yet. It appears that in Asia ILC and/or CEPC may soon be approved
6) BNCT is an important new utensil for accelerator-based medical treatment
7) Small machine: Figure 8 ring, cSTART, PERLE, beam chaser

Technology & physics development

1) Future topics: resume crystalline beam@ESR, Quantum computer on storage ring
2) Overarching themes: 3D printing of spares and a full accelerator
3) Highest field accelerator magnets, fast ramping (600T/s).
4) More efficient positron sources, ERL
5) SRF, FFA development
6) Advanced diagnostics.
7) Laser beam manipulation.
8) Plasma-wake field acceleration
9) Solid states amplifier technology (super reliable!)
10) Energy storage power supply
11) Virtual accelerator (virtual twin)
12) Artificial intelligence, machine learning
    a. Semi-autonomic Operation/ pattern detection/automation
    b. Data analysis/image deconvolution/pattern detection/
    c. Optimization
    d. Language model (chatgpt,….)
    e. Long term
        1) Autonomous accelerator operation
        2) Virtual expert

Megatrends

13) Economic and environmental sustainability
14) Advanced manufacturing
15) A.I.
16) HTS is advancing fast

Interdisciplinary (quantum computing, medical)

Annex B: Photographs from iBiF2024

Figures 58 presents four snapshots from the iFAST iBiF 2024 roadmap workshop.

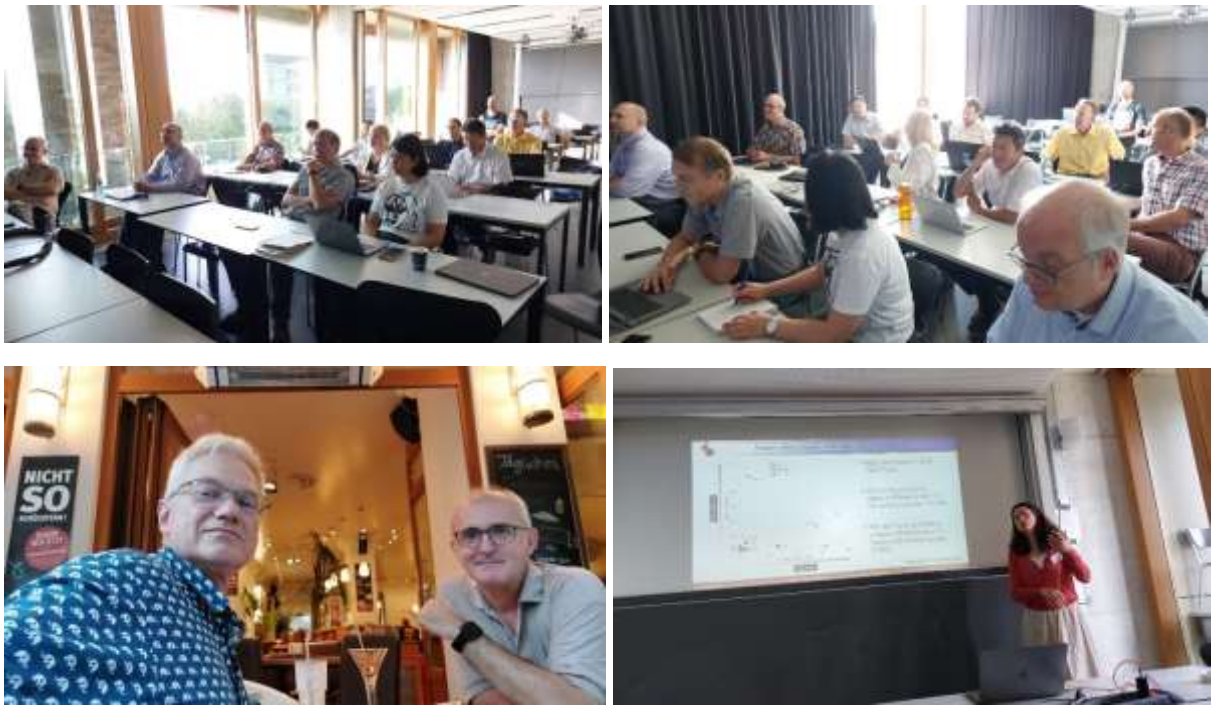

Figure 58 : A few photographs from iBiF2024 in Frankfurt.